AD-A059 690   DAVID W TAYLOR NAVAL SHIP RESEARCH AND DEVELOPMENT CE--ETC F/G 13/10
                TAKEOFF EXPERIMENTS OF A HIGH SPEED HYDROFOIL SYSTEM (TAP-2).(U)
                JUN 75   H D HOLLING
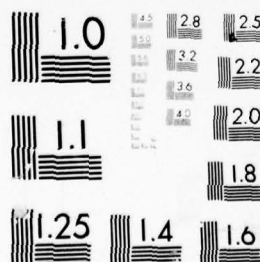UNCLASSIFIED   DTNSRDC/SPD-575-04   NL

1 OF 1
AD
A059690

END
DATE
FILMED
12-78
DDC

AD
ADA059690

	1.0		2.8		2.5
					2.2
	1.1				2.0
					1.8
	1.25		1.4		1.6

MICROCOPY RESOLUTION TEST CHART
NATIONAL BUREAU OF STANDARDS-1963-A

LEVEL (8)

DAVID W. TAYLOR NAVAL SHIP
RESEARCH AND DEVELOPMENT CENTER

Bethesda, Md. 20084

(9) Final rept.,

(6) TAKEOFF EXPERIMENTS OF A HIGH SPEED HYDROFOIL SYSTEM (TAP-2).

by

(10) Henry D. Holling

(12) 81p.

APPROVED FOR PUBLIC RELEASE: DISTRIBUTION UNLIMITED

SHIP PERFORMANCE DEPARTMENT

(11) June 1975

(14) DTNSRDC/SPD-575-04

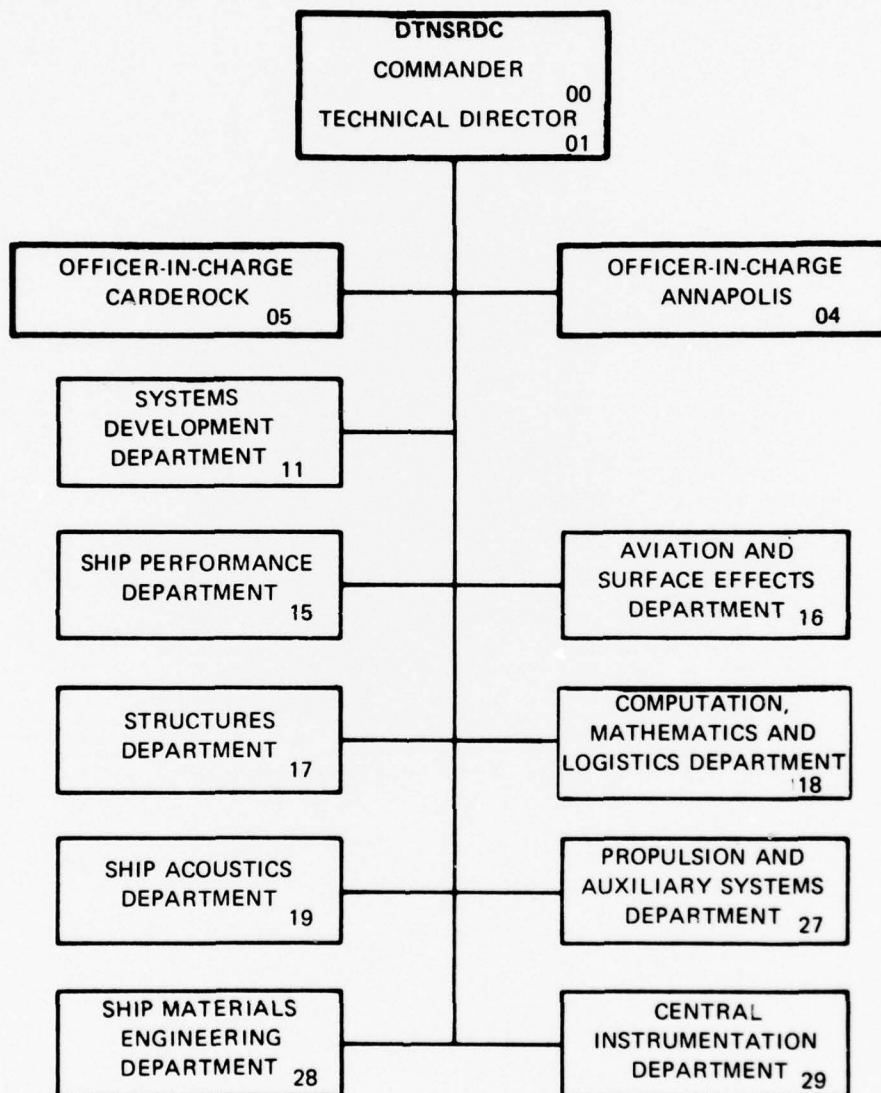389 694   78 10 06 003

MAJOR DTNSRDC ORGANIZATIONAL COMPONENTS

```
                          ┌─────────────────────┐
                          │      DTNSRDC        │
                          │    COMMANDER        │
                          │               00    │
                          │ TECHNICAL DIRECTOR  │
                          │               01    │
                          └─────────────────────┘
                                     │
        ┌──────────────────────┐     │     ┌──────────────────────┐
        │ OFFICER-IN-CHARGE     │     │     │ OFFICER-IN-CHARGE     │
        │ CARDEROCK        05   ├─────┼─────┤ ANNAPOLIS        04   │
        └──────────────────────┘     │     └──────────────────────┘
        ┌──────────────────────┐     │
        │ SYSTEMS              │     │
        │ DEVELOPMENT          ├─────┤
        │ DEPARTMENT    11     │     │
        └──────────────────────┘     │
        ┌──────────────────────┐     │     ┌──────────────────────┐
        │ SHIP PERFORMANCE     │     │     │ AVIATION AND          │
        │ DEPARTMENT           ├─────┼─────┤ SURFACE EFFECTS       │
        │              15      │     │     │ DEPARTMENT     16     │
        └──────────────────────┘     │     └──────────────────────┘
        ┌──────────────────────┐     │     ┌──────────────────────┐
        │ STRUCTURES           │     │     │ COMPUTATION,          │
        │ DEPARTMENT           ├─────┼─────┤ MATHEMATICS AND       │
        │              17      │     │     │ LOGISTICS DEPARTMENT 18│
        └──────────────────────┘     │     └──────────────────────┘
        ┌──────────────────────┐     │     ┌──────────────────────┐
        │ SHIP ACOUSTICS       │     │     │ PROPULSION AND        │
        │ DEPARTMENT           ├─────┼─────┤ AUXILIARY SYSTEMS     │
        │              19      │     │     │ DEPARTMENT     27     │
        └──────────────────────┘     │     └──────────────────────┘
        ┌──────────────────────┐     │     ┌──────────────────────┐
        │ SHIP MATERIALS       │     │     │ CENTRAL               │
        │ ENGINEERING          ├─────┴─────┤ INSTRUMENTATION       │
        │ DEPARTMENT     28    │           │ DEPARTMENT     29     │
        └──────────────────────┘           └──────────────────────┘
```

REPORT DOCUMENTATION PAGE		READ INSTRUCTIONS BEFORE COMPLETING FORM
1. REPORT NUMBER NSRDC SPD-575-04 ✓	2. GOVT ACCESSION NO.	3. RECIPIENT'S CATALOG NUMBER
4. TITLE *(and Subtitle)* TAKEOFF EXPERIMENTS OF A HIGH SPEED HYDROFOIL SYSTEM (TAP-2)		5. TYPE OF REPORT & PERIOD COVERED Final
		6. PERFORMING ORG. REPORT NUMBER
7. AUTHOR(s) Henry D. Holling		8. CONTRACT OR GRANT NUMBER(s)
9. PERFORMING ORGANIZATION NAME AND ADDRESS Naval Ship Research and Development Center Bethesda, Maryland 20084		10. PROGRAM ELEMENT, PROJECT, TASK AREA & WORK UNIT NUMBERS
11. CONTROLLING OFFICE NAME AND ADDRESS		12. REPORT DATE June 1975
		13. NUMBER OF PAGES 78
14. MONITORING AGENCY NAME & ADDRESS(*If different from Controlling Office*)		15. SECURITY CLASS. *(of this report)*
		15a. DECLASSIFICATION DOWNGRADING SCHEDULE

16. DISTRIBUTION STATEMENT *(of this Report)*

APPROVED FOR PUBLIC RELEASE: DISTRIBUTION UNLIMITED

17. DISTRIBUTION STATEMENT *(of the abstract entered in Block 20, if different from Report)*

18. SUPPLEMENTARY NOTES

19. KEY WORDS *(Continue on reverse side if necessary and identify by block number)*

Hydrofoils, Hydrofoil Takeoff, Hydrofoil Struts, High Aspect Ratio Hydrofoils

20. ABSTRACT *(Continue on reverse side if necessary and identify by block number)*

As part of an effort to develop a data base and design criterion for high speed struts and foils, experiments were conducted to evaluate the TAP-2 foil performance for a range of speeds, including the design takeoff speed of 35 knots. The T-foil system, designated as TAP-2, was designed to operate fully wetted at takeoff and as a supercavitating foil at a 60 knot cruise speed. ——> over

DD _{1 JAN 73} FORM 1473 EDITION OF 1 NOV 65 IS OBSOLETE
S/N 0102-014-6601

Experiments were conducted at 30, 35, 40, 45, and 50 knots at various depth-to-chord ratios and at a range of foil incidence angles.

The maximum lift coefficient for the foil system was found to be $C_L = 0.738$ at 30 knots - the lowest speed run in the evaluation. At the takeoff speed of 35 knots and $d/c' = 2.0$, the maximum lift coefficient was 0.534 and the maximum L/D was 14.25.

TABLE OF CONTENTS

iii

LIST OF FIGURES

iv

LIST OF FIGURES - Continued

LIST OF TABLES

v

NOTATION

A	Foil plan area	ft^2
C_D	Drag coefficient of strut/foil configuration, $C_D = D/[1/2\rho V^2 A]$	nondimensional
C_L	Lift coefficient of strut/foil configuration, $C_L = L/[1/2\rho V^2 A]$	nondimensional
C_M	Pitching moment coefficient of strut/foil configuration about the pitch center of the dynamometer, $C_M = M/[1/2\rho V^2 Ac']$	nondimensional
c	Foil chord length	in.
c'	Mean foil chord length (average of centerline and tip chord lengths including flap)	in.
D	Drag of strut/foil configuration	lb
d	Foil depth from still water surface	in.
d'	Strut depth from still water surface	in.
d/c'	Strut/foil depth-to-chord ratio	nondimensional
d'/c'	Bare strut depth-to-chord ratio	nondimensional
F_n	Froude number, strut/foil configuration $F_n = V/\sqrt{gc'}$	nondimensional
g	Acceleration due to gravity	ft/sec^2
L	Lift of strut/foil configuration	lb
L/D	Lift-to-drag ratio of strut/foil configuration	nondimensional

M	Pitching moment of strut/foil configuration about the pitch center of the dynamometer	in-lb
p_V	Experimental facility water vapor pressure	lb/ft^2
p_∞	Free stream static pressure	lb/ft^2
R_n	Reynolds number, $R_n = Vc'/\nu$ for the strut/foil configuration $R_n = Vs'/\nu$ for the bare strut configuration	nondimensional
s'	Swept strut chord length at the still water interface	in.
V	Velocity	knots and ft/sec
X	Fractional chord length	nondimensional
α	Foil incidence angle referenced to the horizontal	deg
β	Strut sweep angle referenced to the vertical	deg
ν	Kinematic viscosity	ft^2/sec
ρ	Water density	$lb\text{-}sec^2/ft^4$
σ	Cavitation number based on fluid vapor pressure, $\sigma = [p_\infty - p_V] / [1/2\rho V^2]$	nondimensional
τ	Local foil section or cavity thickness	in.
τ/c	Local thickness-to-chord ratio	nondimensional

ABSTRACT

As part of an effort to develop a data base and design criterion for high speed struts and foils, experiments were conducted to evaluate the TAP-2 foil performance for a range of speeds, including the design takeoff speed of 35 knots. The T-foil system, designated as TAP-2, was designed to operate fully wetted at takeoff and as a supercavitating foil at a 60 knot cruise speed.

Experiments were conducted at 30, 35, 40, 45, and 50 knots at various depth-to-chord ratios and at a range of foil incidence angles.

The maximum lift coefficient for the foil system was found to be C_L = 0.738 at 30 knots - the lowest speed run in the evaluation. At the takeoff speed of 35 knots and d/c' = 2.0, the maximum lift coefficient was 0.534 and the maximum L/D was 14.25.

ADMINISTRATIVE INFORMATION

INTRODUCTION

In September 1972, the Naval Material Command tasked the Naval Ship Research and Development Center to develop a data base and design criterion for high speed struts and foils in general and the Developmental Fast Hydrofoil (DFH) in particular. The procedures selected to accomplish the primary objectives have been to:

1. Select strut/foil configurations for high speed operation,

2. Determine hydrodynamic loads for strut/foil systems associated with their various operational modes,

3. Determine methods of controlling these hydrodynamic loads, and

4. Determine the impact of hydrodynamic loadings on structures and materials.

As part of this program, takeoff experiments were conducted in Langley Tank No. 1 of NSRDC with a foil system designated as TAP-2. The foil had been designed[1] using Furuya's[2] prediction program for supercavitating foil sections operating beneath a free water surface. The purpose of these experiments was to determine lift and drag forces, foil pitching moments, and cavitation characteristics of the strut/foil system at various depths.

---

[1] Baker, Elwyn S., "Design of Hydrofoil TAP-2," NSRDC SPD Report 575-03 (June 1975)

[2] Furuya, Okitsugu, "Nonlinear Calculations of Arbitrarily Shaped Supercavitating Hydrofoils Near a Free Surface," Journal of Fluid Mechanics, Vol. 68, Part 1 (March 1975)

DESCRIPTION OF MODEL

The foil system to be evaluated was designed such that it would operate fully wetted at takeoff and as a supercavitating foil at 60 knots. A large aspect ratio which would give a high lift component was desirable since the foil would operate fully wetted at takeoff. A spanwise taper (tip chord/root chord = 0.5) was included in the design to reduce stresses in the foil leading edge.

The high speed foil design was based on use of Furuya's performance prediction program for supercavitating foil sections beneath a free water surface. This program assumes that the lower surface profile is comprised of a leading edge ellipse (i.e. blunt nosed section) with the remainder of the lower surface profile being a circular arc.

The foil upper surface (suction side) was generated such that the surface at each section lay beneath the predicted location of the free streamline. Clearance between the upper surface and the cavity interface was designed to be minimal near the foil leading edge (where the shape of the cavity is known) and substantial (>20% of predicted cavity thickness) at the foil trailing edge. Assuming given lower surface geometry and predicted cavity thickness the section upper surface was generated from the expression

$$(\tau/c)_{foil} = 0.80 \ (1.25 - 0.25X) \ (\tau/c)_{cavity}$$

3

where X is the fraction of chord length from the foil section leading edge. From 70% to 100% chord the foil thickness was further reduced by a circular arc fairing from the 70% chord point to the trailing edge flap.

The TAP-2 foil was constructed with a trailing edge flap to generate additional lift capability during takeoff. The flap area was approximately 20% of the foil area.

Photographs and sketches of the TAP-2 strut-foil model are shown in Figures 1, 2, and 3. Foil geometry characteristics are listed in Table 1. Characteristic dimensions shown in Figure 2 include the flap section.

The support strut had a chord length of 6 inches and a span of 29 inches. The strut section was a NACA 16-012 airfoil shape. Section offsets and geometry are shown in Figure 4.

The basic TAP-2 foil was constructed with blunt wing tips. At the conclusion of the experimental program with the basic configuration the foil tips were modified to investigate tip shape effects on foil drag. The tips were rounded by cutting circles tangent to the upper and lower foil surfaces at stations along the chord.

EXPERIMENTAL APPARATUS AND PROCEDURE

Hydrofoil takeoff experiments were conducted on the towing carriage at Langley Tank 1. A detailed description of the facility

4

can be found in Reference 3. The hydrofoil was mounted through its support strut to a bracket (see Figure 5) and in turn to a six-component dynamometer. The dynamometer was attached to an elevator designed for and permanently fixed to the carriage. The elevator has a vertical travel of 27 inches with the dynamometer attached. The dynamometer can be configured for high or low ranges. For these experiments the high load range of lift ($\pm$ 2250 lbs), low range of drag (-150 lbs) and high range of pitching moment (46,800 in-lb) were used.

Model experiments were conducted at 30, 35, 40, 45 and 50 knots at various depth-to-chord ratios and for a range of incidence angles. At the conclusion of these experiments, the foil tips were faired as previously described and experiments were repeated to determine if tip vortex cavitation characteristics would be altered and if consequent changes to lift and drag would result. After all foil experiments were completed, runs were made with the bare strut at various speeds at $d'/c' = 1.0$, 2.0, and 3.0 and strut sweep angle of -9 degrees.

Foil chord length referenced in this text includes the chord line from the leading edge of the foil to the trailing edge of the flap. Foil section incidence angle was constant along the foil span and was

---

[3] Olson, R. E. and W. F. Brownell, "Facilities and Research Capabilities, High Speed Phenomena Division, David Taylor Model Basin, Langley Field, Va." DTMB Report 1809 (April 1964)

defined as the geometric angle between the foil chord and the horizontal reference plane. Foil incidence was set by matching precise holes in the strut and strut support bracket (Figure 5) and securing with pins. This allowed foil angle of attack adjustment in one degree increments up to +11.814 degrees. A table indicating hole number on the strut support bracket in relation to strut angle (referenced to the vertical) and foil incidence angle is given in Table 2. The relationship between the strut sweep angle and foil incidence angle is given by α = constant + β where β is the strut sweep angle with the vertical. The constant value of 11.814 degrees is a constructed angle between the strut chord line and the foil chord line (see Figure 5).

Foil depth was set and checked before each run. The reference point used in determining depth below the water surface was a point on the leading edge of the foil mean chord section. Strut depth for the bare strut runs was based on the foil mean chord and was referenced to the leading edge at the bottom surface of the strut. A complete outline of conditions set during the takeoff experiments is included in Table 3.

Lift, drag, pitching moment, and speed were recorded with a digital data collection system and data analyses were performed on line with a mini-computer. Pitching moment was referenced to the moment center of the dynamometer (see Figure 5). One to four (depending on speed) three-second data samples were collected for

6

each speed run. The data were averaged during the collection time.
In the analyses, presented data were the average of each collected
sample.

Closed circuit television, motion pictures, above water and
underwater still photographs were taken and used for recording
cavitation characteristics observed during the experiments.

DATA ACCURACY

It was the aim of the program to run experimental conditions
at 30, 35, 40, 45, and 50 knots. An examination of all recorded
speeds (three-second averages) showed that the average velocity
differential from the desired speed was 0.8 percent. The average
variation in speed from the first data sample to the second data
sample during a given carriage run was 0.6 percent. All coefficient
data presented in this report, which were nondimensionalized on
velocity, were calculated using the average force, moment, and
speed values obtained during the data sampling periods. The area
used in the coefficient calculations was the total area of the foil
including the flap area. The cavitation number, σ, values reported
in Table 4 are based on the mean values of speed.

The accuracy in setting the geometric foil incidence angle was
$\pm$ 0.05 degree. The dimension locating the dynamometer moment center
with respect to the strut pivot point (Figure 5) was correct to
within $\pm$ 0.1 inch.

The dynamometer arrangement used in the experiment was comprised of modular force gages. Two gages rated to 3000 pounds (axially spaced 36 inches apart) made up the lift and pitching moment sensors and one 230 pound rated gage carried the drag force. The accuracy of these modular force gages is considered to be $\pm$ 0.5 percent of their full scale rated load.

The average water temperature throughout the experiments was 46 degrees and was within $\pm$ 2.0 degrees of that value for the period of experimentation and for the extent of the basin. The specific gravity of the water was 1.014 and density, ρ, was 1.9682 lb-sec^2/ft^4.

DATA REDUCTION

Lift and drag forces were measured normal and parallel, respectively, to the horizontal plane. The lift coefficient is defined by

$$C_L = \frac{L}{1/2 \rho V^2 A}$$

where A is the foil plan area including the flap area. The drag coefficient is defined by

$$C_D = \frac{D}{1/2 \rho V^2 A}$$

Drag is defined as the total strut and foil drag. For consistency, this formulation was also used for generating the bare strut drag coefficient data. The pitching moment is referenced to the moment

8

center of the dynamometer and pitching moment coefficient is defined as

$$C_M = \frac{M}{1/2\rho V^2 A c'}$$

where c' is the mean foil (including flap) chord length.

Cavity pressure was not measured, however, cavitation numbers for vapor cavities were computed as

$$\sigma = \frac{p_\infty - p_V}{1/2\rho V^2}$$

where p_∞ was free stream static pressure in pounds per square foot, p_V was ambient fluid vapor pressure in pounds per square foot.

Froude number for the foil experiments was defined by

$$F_n = \frac{V}{\sqrt{gc'}}$$

where c' = mean chord length and g = acceleration due to gravity.

Reynolds number for the strut/foil configuration was defined as

$$R_n = \frac{Vc'}{\nu}$$

where ν was the kinematic viscosity of the tank water at the average water temperature and assumed to have the value of 1.529×10^{-5} ft^2/sec throughout the experiments.

9

For the bare strut experiments, Reynolds number was defined as

$$R_n = \frac{Vs'}{\nu}$$

where s' = the swept strut chord length at the still water interface.

RESULTS

Experimental data for the TAP-2 strut/foil configuration are presented graphically and in tabular form. Lift and drag coefficients and lift-to-drag ratios are plotted as functions of foil incidence angle showing effects of carriage velocity and foil submergence. Lift and drag coefficient data have also been plotted as functions of carraige velocity showing the effects of foil angle of attack. Drag coefficient data for the bare strut runs have been plotted as a function of Reynolds number. All data have been tabulated and are presented in Table 3.

Figure 6 presents lift and drag coefficient data plotted at velocities corresponding to the experimental condition. Separate plots are shown for depth-to-chord ratios of 1.0, 2.0, and 3.0. A rather detailed legend has been compiled for Figure 6 which depicts the type or types of cavitation existing at the given experimental condition. In instances where cavitation of a given type was slight, the speed condition has been noted in parentheses and consequently gives an indication of the point of cavitation

10

inception. The schematic shown in Figure 7 depicts the areas of the foil, i.e., pressure side, suction side, leading and trailing edges, along span and in the vicinity of the strut, in which cavitation was observed on the photographs. In all areas there were no apparent differences in cavitation patterns between the basic strut/foil configuration and the configuration with modified foil tips.

Figures 8 and 9 show representative photographs obtained for the basic configuration at various carriage velocities, foil incidence angles and submergence depths. The photographs appear in two sections; one section shows above water photographs of the foil suction side with cavitation associated with the given experimental condition. The remainder of the photographs are underwater pictures of the foil lower surface identified as the normal pressure side of the foil.

Figures 10 through 18 show lift coefficients, drag coefficients, and lift-to-drag ratios for a variation in foil incidence angle. Different plots are included for the different foil submergence conditions. Since it has been previously noted that carriage velocity varied slightly (up to 0.8 percent) from the prescribed values of 30, 35, 40, 45, and 50 knots, curves indicating velocity must be considered approximate. The faired curves connecting symbols for a given velocity condition have been superimposed on

11

the plots as a visual aid and do not represent any mathematically defined data fit procedure. Any nondimensional coefficients presented, however, were calculated using the exact velocity measured during a data sampling period. The data in Figures 10 to 18 show that lift coefficient increased with increasing foil incidence angle but decreased with increasing speed at constant foil incidence angle. Drag coefficient curves displayed minimal values within the range of experimental conditions and were generally at a minimum at small (positive or negative) foil incidence angles. The incidence angle values which corresponded to conditions of minimum drag coefficient showed some dependence on velocity and, therefore, involved effects of cavitation, submergence, and flow characteristics on the strut at the water surface.

The maximum L/D which was obtained for the conditions evaluated at $d/c' = 1.0$ was 10.7 at an $\alpha = 2.814$ and V = 40 knots. At depth-to-chord ratios of 2.0 and 3.0, L/D values were near 14.0 at foil incidence angles near 1.0 degrees and at V = 35 knots.

Figures 19 through 22 show lift and drag coefficients versus foil incidence angle. Experimental results for conditions at varying foil submergences are superimposed on the plots. At a given speed the lift and drag coefficients show little variation with submergence at d/c' values of 2.0 and 3.0. Comparisons of these coefficient data with those corresponding to the $d/c' = 1.0$ show slight reductions in the drag coefficients at the shallow

12

condition which can be attributed to the reduced wetted strut area.

Drag coefficients obtained in the bare strut experiments are shown in Figure 23. These are plotted versus a Reynolds number based on the swept strut chord length at the still water interface. For these experiments the strut tip was submerged 5.4 inches, 10.8 inches, and 16.2 inches corresponding to one, two, and three times the characteristic length of the foil mean chord. Drag coefficients shown in Figure 23 were mean values of 2 to 6 data samples. The average scatter for these data was ± 30% of the mean value.

Froude number, Reynolds numbers, and cavitation numbers calculated for each experimental condition for the strut/foil configuration and for the bare strut where applicable have been given in Tables 3 and 4.

CONCLUSIONS

1. Large lift-to-drag ratios were achieved at takeoff conditions for the TAP-2 foil/strut configuration. Lift-to-drag ratios near 14.0 were measured at certain combinations of speed, foil incidence angle, and foil submergence.

2. Lift coefficient increased with increasing incidence angle at constant speed but decreased with increasing speed at constant incidence angles.

3. Rounding the foil wing tips had no significant effect on foil lift or drag and there was no apparent change in tip vortex cavitation.

13

4. Foil submergence change had little effect on lift and drag coefficients at depth-to-chord ratios of 2.0 and 3.0. Nearer the surface at d/c' = 1.0, drag coefficients were less than comparable values obtained at greater depths. Some of the reduction is attributable to the reduced strut wetted area.

5. TAP-2 pressure side (bottom) and suction side (top) surfaces were subject to cavitation at different locations on the surfaces depending on velocity and foil incidence angle. In general, the foil pressure side was fully wetted at incidence angles of 3.814 and greater for all speeds. Pressure side cavitation, when occurring at small positive and all negative incidence angles, tended to begin at the foil centerplane. Suction side cavitation occurred along the span of the foil leading edge at high incidence angles (i.e. 4.814 - 6.814). Cavitation near the strut trailing edge was common for most conditions. Suction side cavitation along the span of the flap occurred and increased in intensity as the angle of attack or speed increased.

6. In general, all cavitation (suction and pressure side) was minimal in extent at a foil incidence angle of 3.814.

REFERENCES

1. Baker, Elwyn S., "Design of Hydrofoil TAP-2," NSRDC SPD Report 575-03 (June 1975)

2. Furuya, Okitsugu, "Nonlinear Calculations of Arbitrarily Shaped Supercavitating Hydrofoils Near a Free Surface," Journal of Fluid Mechanics, Vol. 68, Part 1 (March 1975).

3. Olson, R.E. and W. F. Brownell, "Facilities and Research Capabilities, High Speed Phenomena Division, David Taylor Model Basin Langley Field, Va." DTMB Report 1809 (April 1964)

14
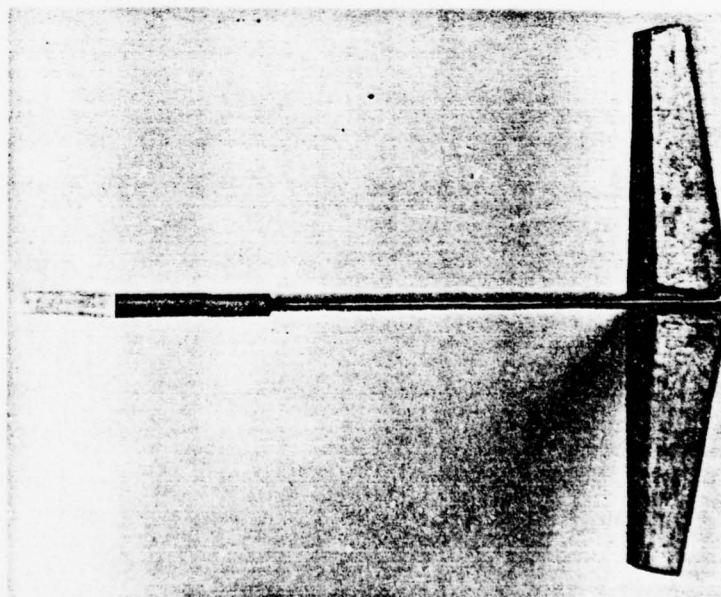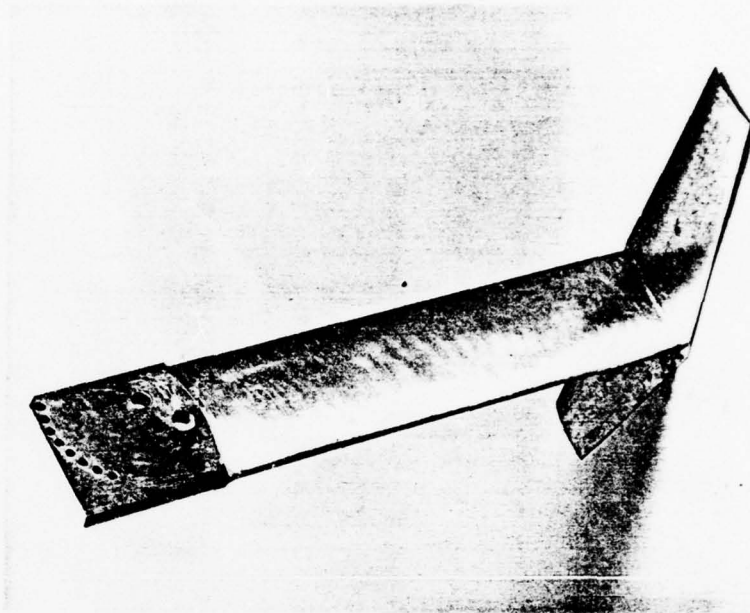
Figure 1 - Photographs of TAP-2 Strut-Foil Model

15

Centerline Chord = 7.20"

Strut Chord = 6.00"

Trailing Edge Flap

Mean Chord = 5.40"

Tip Chord = 3.60"

22.50"

5.625"
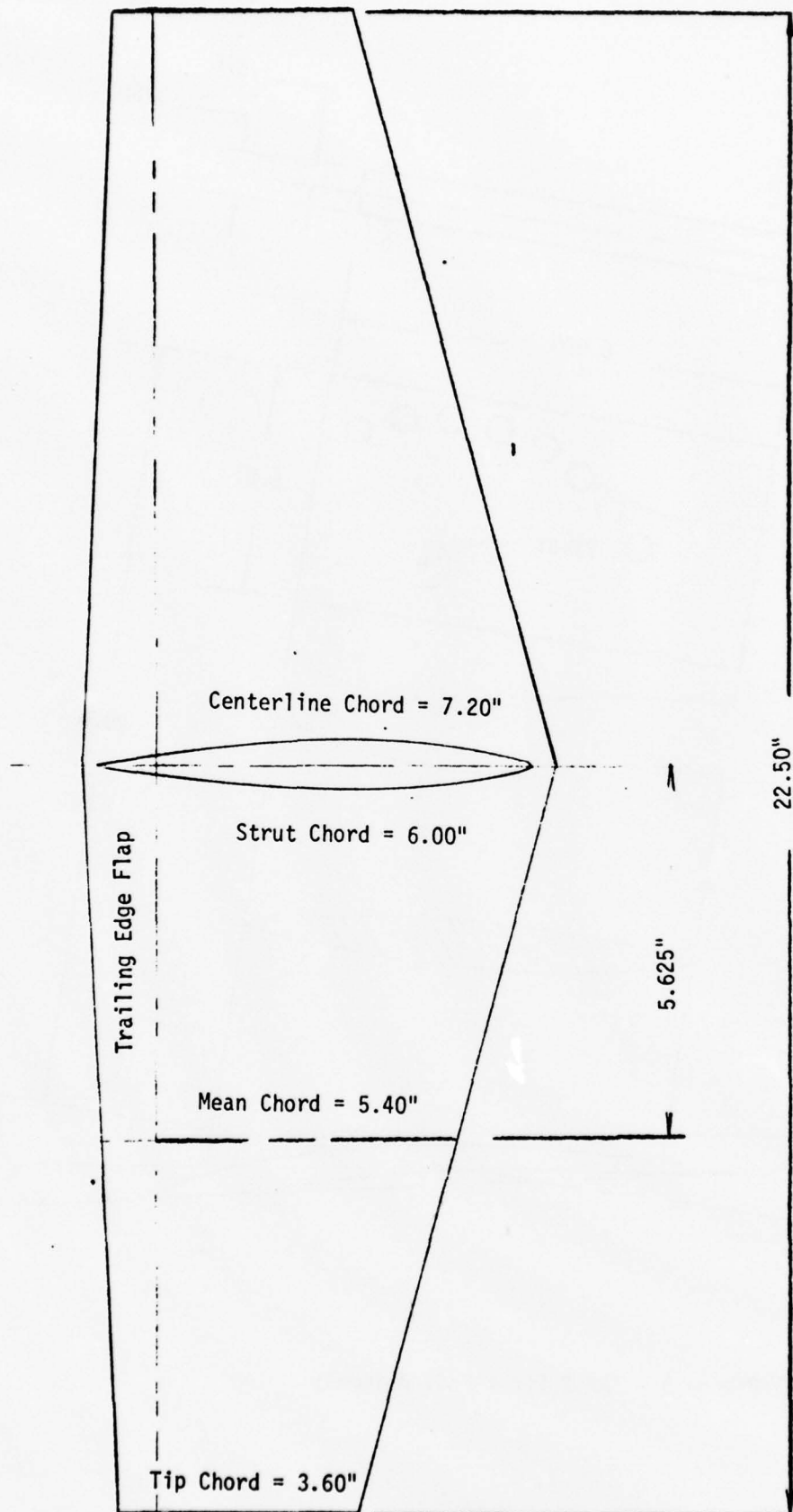
Figure 2 - TAP-2 Foil, Plan View

16
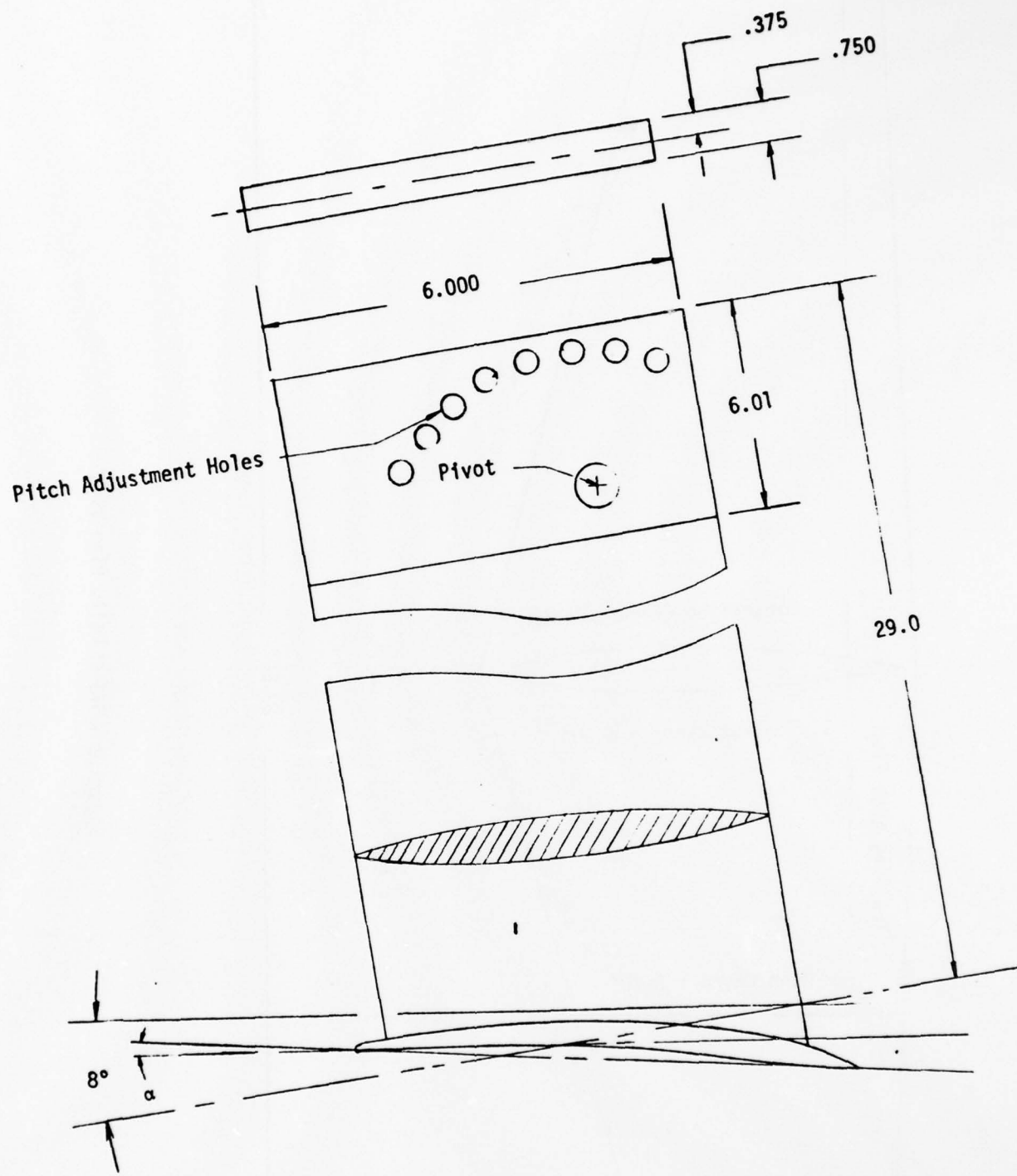
Figure 3 - TAP-2 Strut-Foil Assembly

17

NACA 16-012 HYDROFOIL STRUT COORDINATES

X	X	Y	Y
% Chord	Inches	% Chord	Inches
0.00	.000	0.000	.0000
1.25	.075	1.292	.0775
2.50	.150	1.805	.1083
5.00	.300	2.509	.1505
7.50	.450	3.032	.1819
10.00	.600	3.457	.2074
15.00	.900	4.135	.2481
20.00	1.200	4.664	.2798
30.00	1.800	5.417	.3250
40.00	2.400	5.855	.3513
50.00	3.000	6.000	.3600
60.00	3.600	5.835	.3501
70.00	4.200	5.269	.3161
80.00	4.800	4.199	.2519
90.00	5.400	2.517	.1510
95.00	5.700	1.415	.0849
100.00	6.000	0.000	.0000

Leading Edge Radius 0.703% of C = .0421 Inches
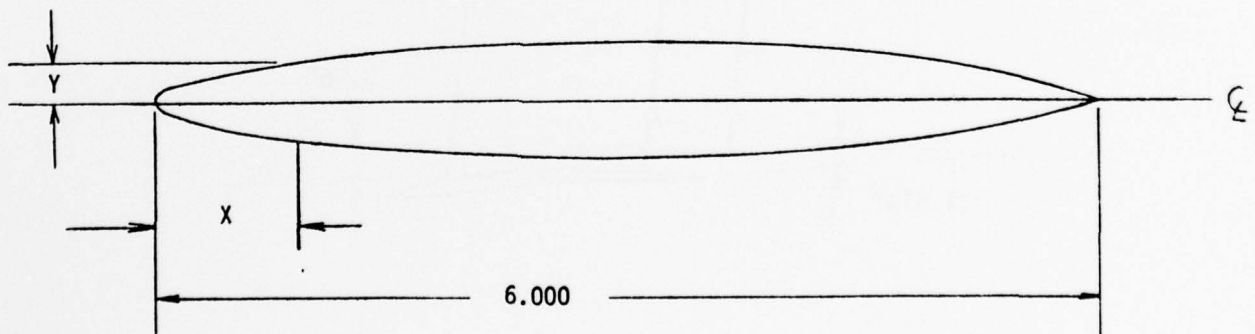
Figure 4 - Schematic and Coordinates of the TAP-2 Strut Section

18
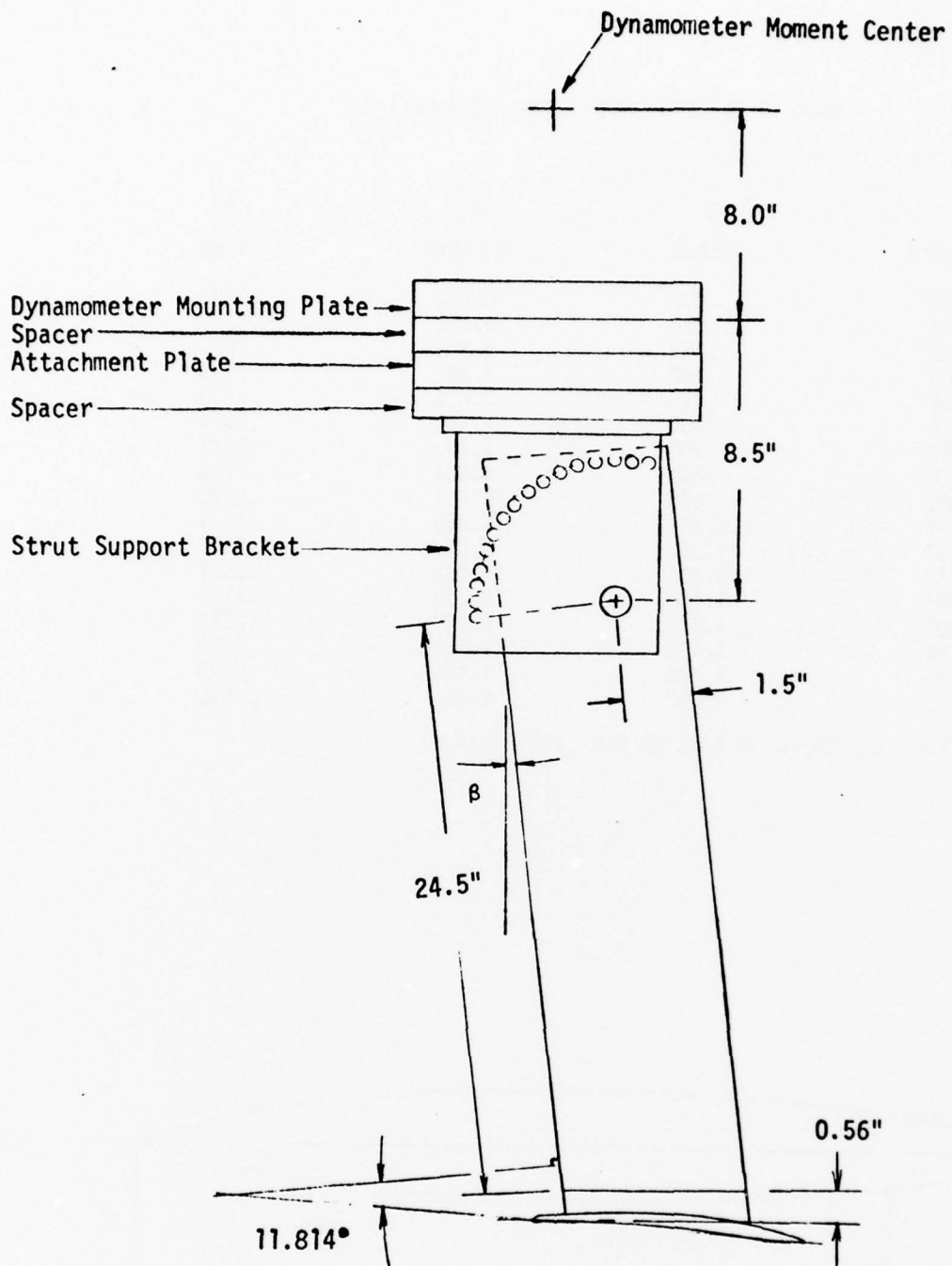
Figure 5 - TAP-2 Foil-Strut Mounting Arrangement

19

LEGEND FOR FIGURE 6
VELOCITIES AT WHICH CAVITATION WAS OBSERVED

Symbol	α	Pressure Side Leading Edge	Suction Side Fully Wetted	Suction Side Leading Edge	On Trailing Edge Flap At Strut and Along Span	On Trailing Edge Flap Only At Strut
				$d/c' = 1.0$		
○	-2.186	40			40	
□	-1.186	40, 45			40, 45	35
◁	-0.186	40 - 50			40 - 50	35
◇	0.814	40 - 50			40 - 50	35
◣	1.814	40 - 50			40 - 50	35
◇	2.814	(40) (45)			40 - 50	35
				$d/c' = 2.0$		
○	-2.186	35, 40			40	
□	-1.186	35, 40			40	
◁	-0.186	30 - 45	30		(35) 40, 45	
◇	0.814	35 - 45	30		(35) 40, 45	
◣	1.814	(35) - 45	30		(35) 40, 45	
◇	2.814	(40), (45)	30		35 - 45	
◁	3.814		30		35	
◢	4.814			(30)		
▷	5.814			30		
▷	6.814			30		
				$d/c' = 3.0$		
○	-2.186	30 - 40	30		40	
□	-1.186	30 - 45	30		40, 45	35
◁	-0.186	30 - 45	30		(35) 40, 45	35
◇	0.814	30 - 45	30		(35) 40, 45	35
◣	1.814	(35) - 45	30		(35) 40, 45	35
◇	2.814		30		35	35
◁	3.814		30		35	
◢	4.814			30		
▷	5.814			30		
▷	6.814			30		

( ) Slight Cavitation   ■ Tip Modification

20

Figure 6 - Lift and Drag Coefficients as a Function of Speed for Various
Foil Incidence Angles at d/c' = 1.0, 2.0, and 3.0

Figure 6 - Continued

22

Figure 6 - Continued

23
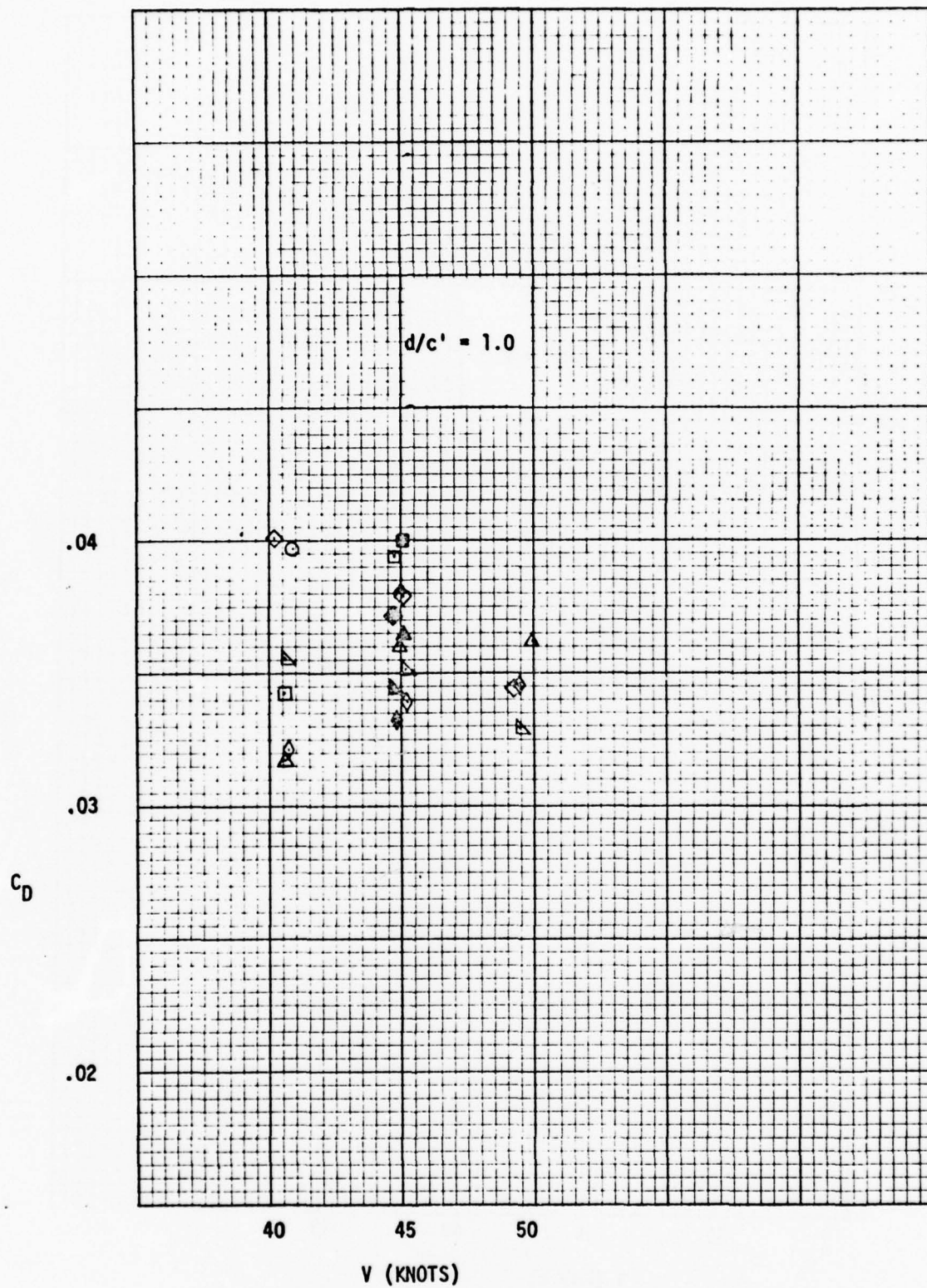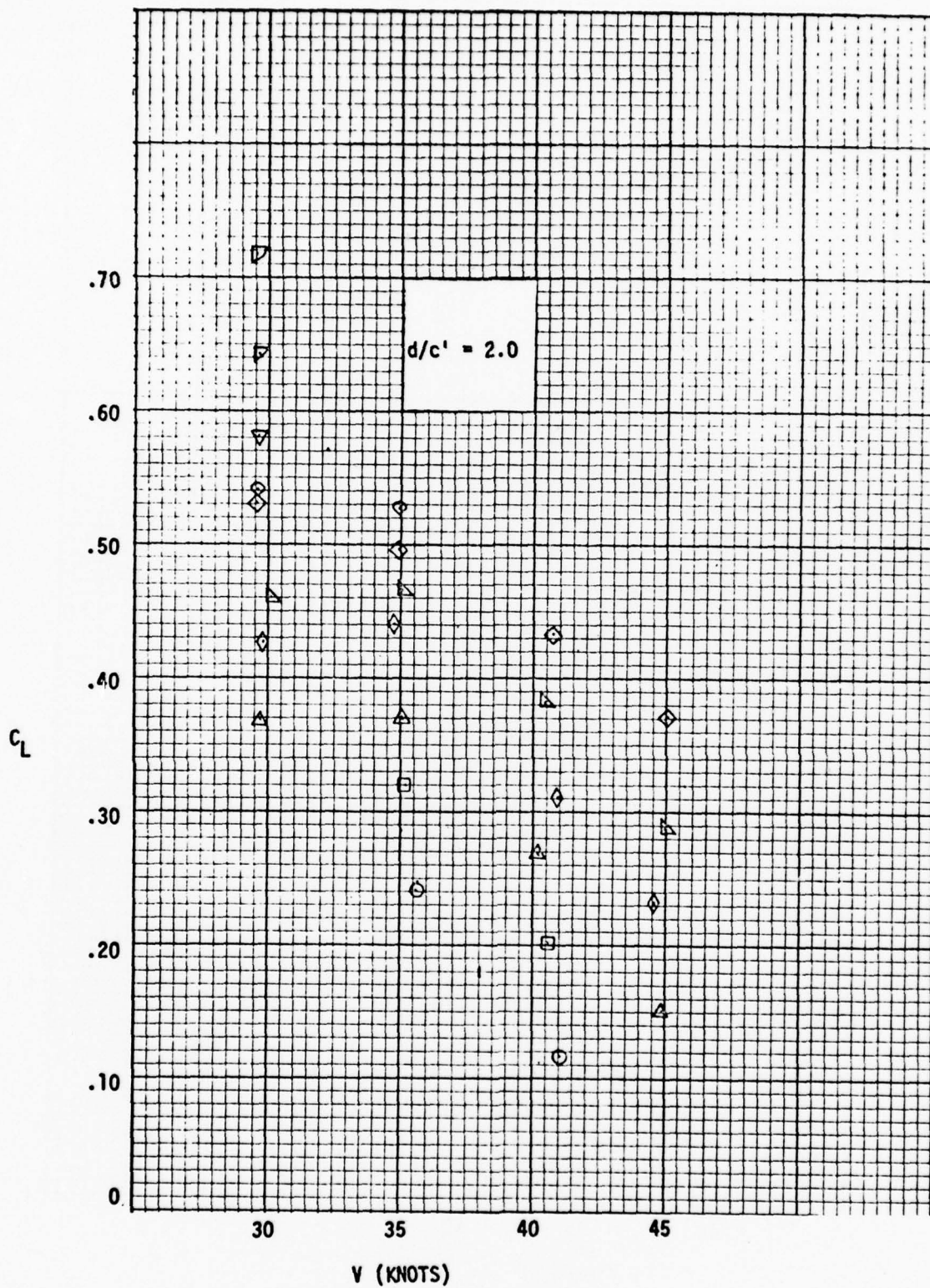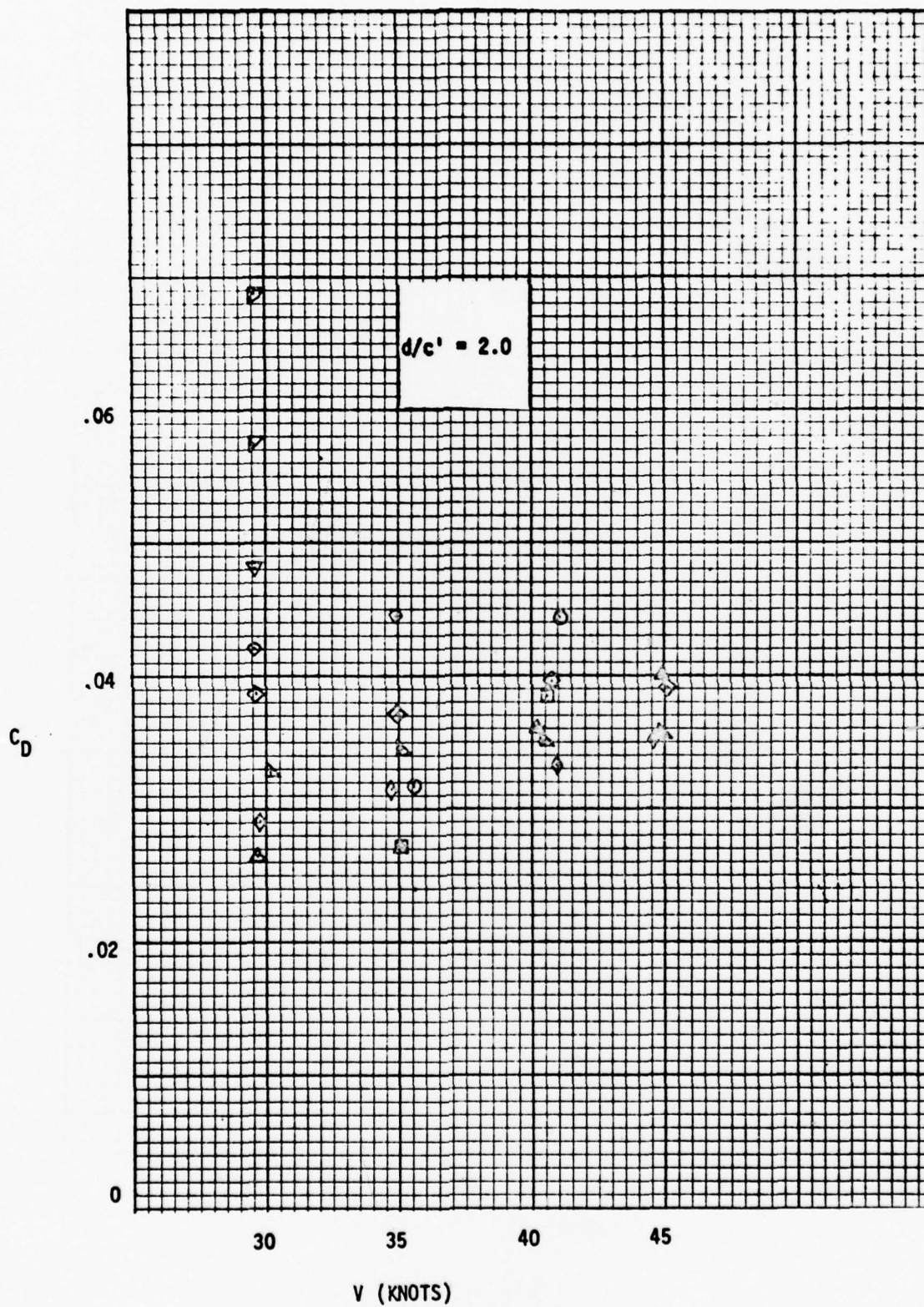
Figure 6 - Continued

24

Figure 6 - Continued

25

Figure 6 - Continued

Trailing Edge Cavitation at Strut

Trailing Edge Cavitation Along Span

Flap

Foil Suction Side

Suction Side Leading Edge Cavitation

Foil Pressure Side

Pressure Side Leading Edge Cavitation

27
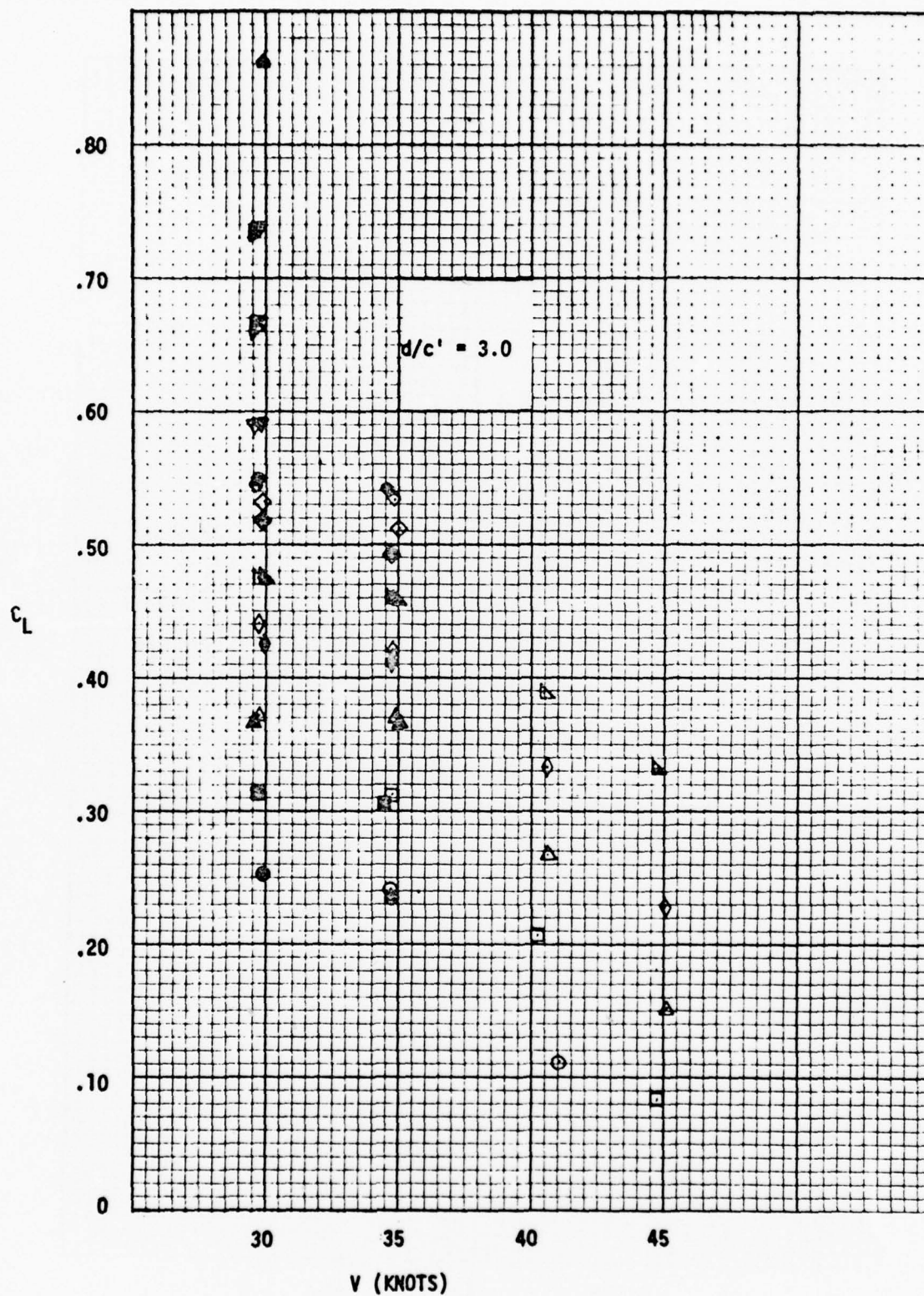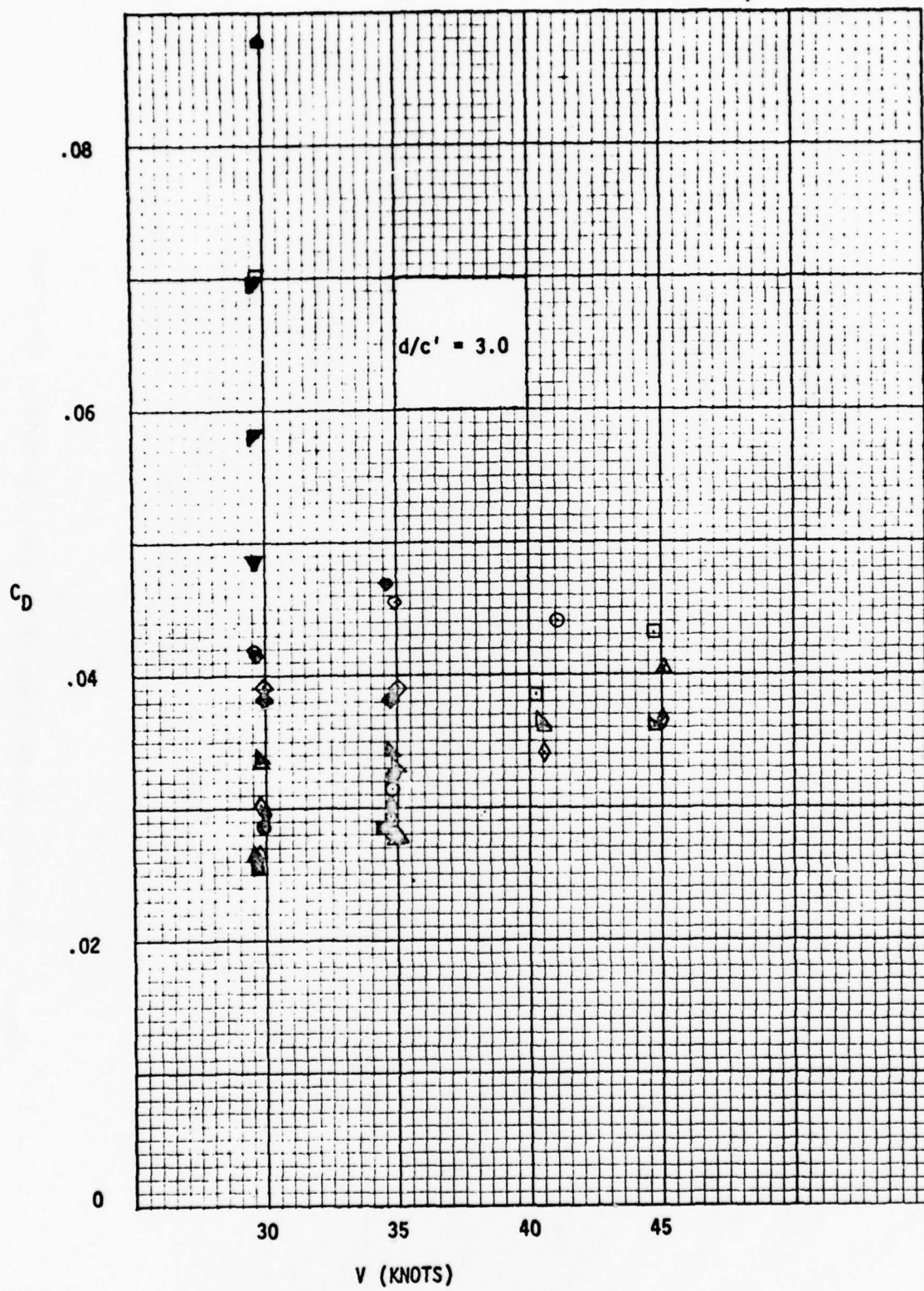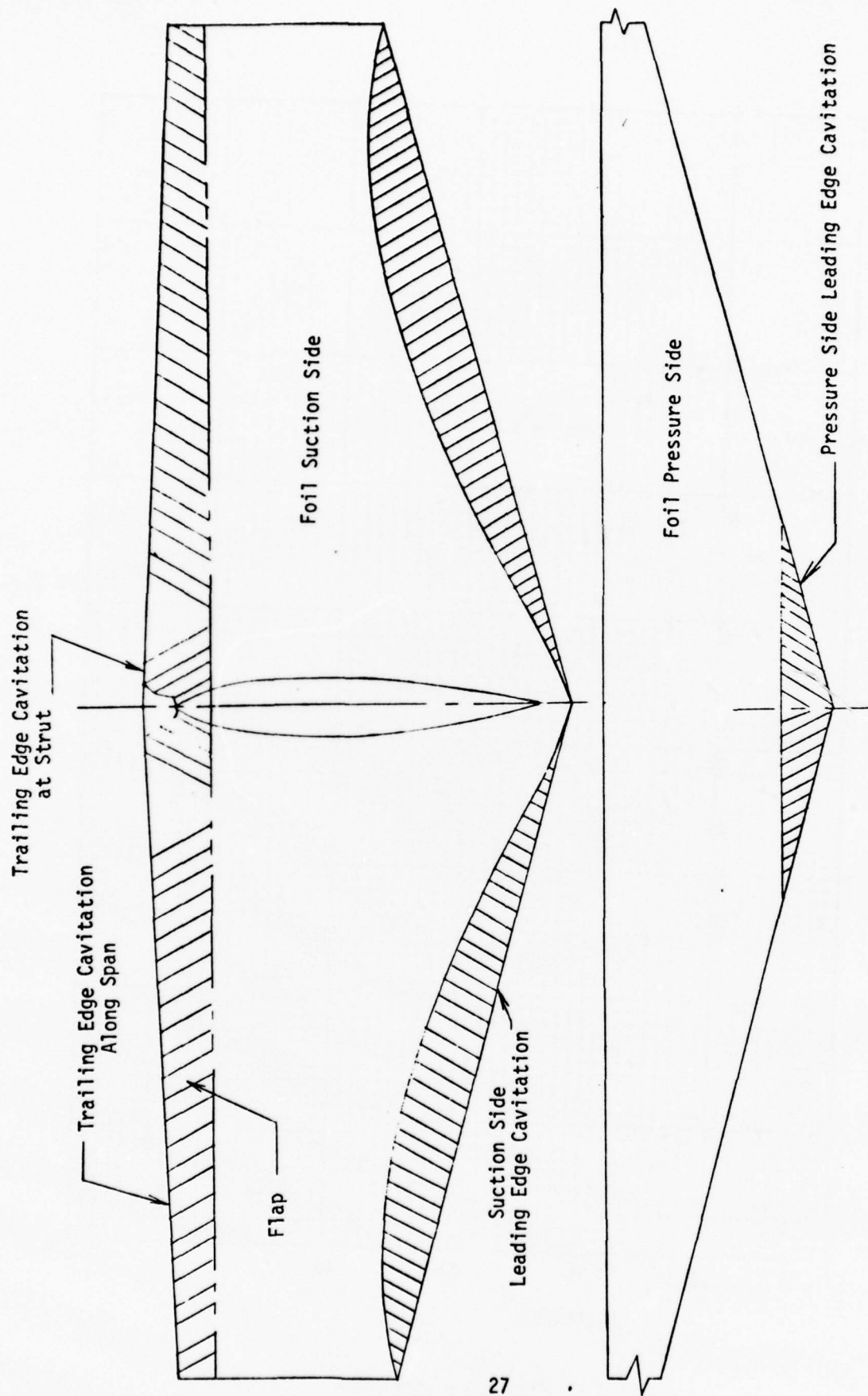
Figure 7 - Schematic Showing Areas of Cavitation Formation; TAP-2 Foil

α = 0.814 deg
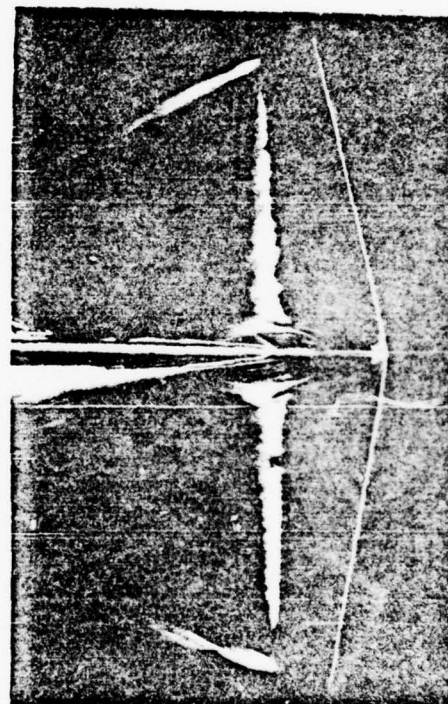
α = 1.814 deg

α = 2.814 deg

Figure 8(a) - V = 40 Knots, d/c' = 1.0

Figure 8 - Above Water Photographs of Suction Side View of TAP-2 Strut-Foil Model
at Various Experimental Conditions

28
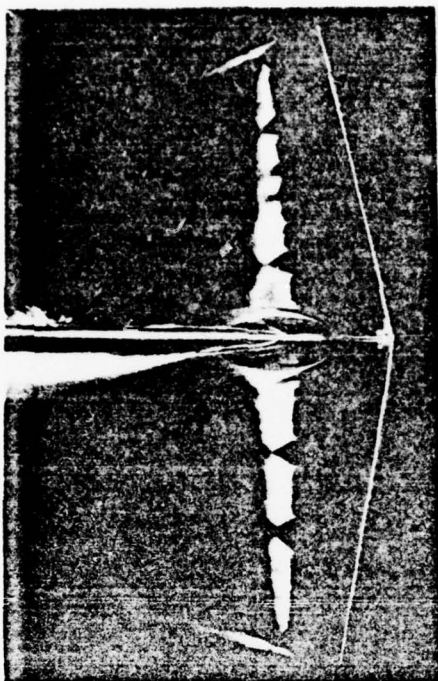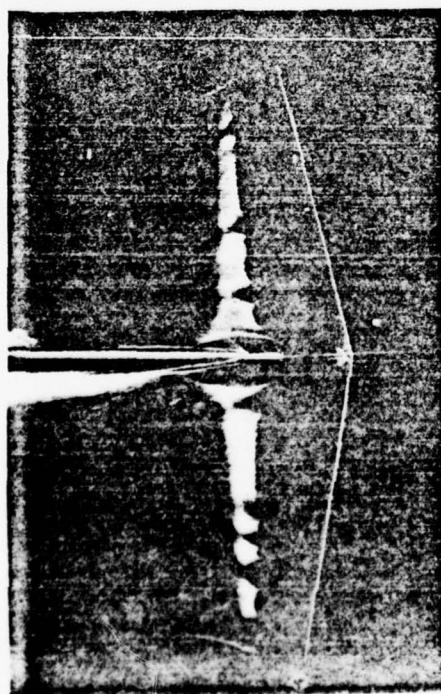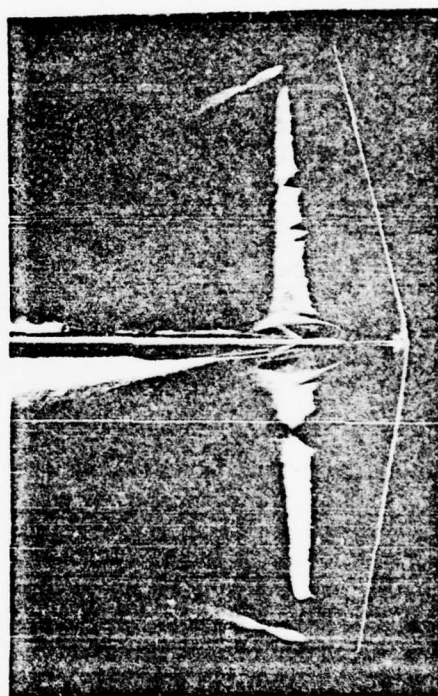
$\alpha = 0.814$ deg

$\alpha = 1.814$ deg

$\alpha = 2.814$ deg

Figure 8(b) - V = 45 Knots, d/c' = 1.0

29
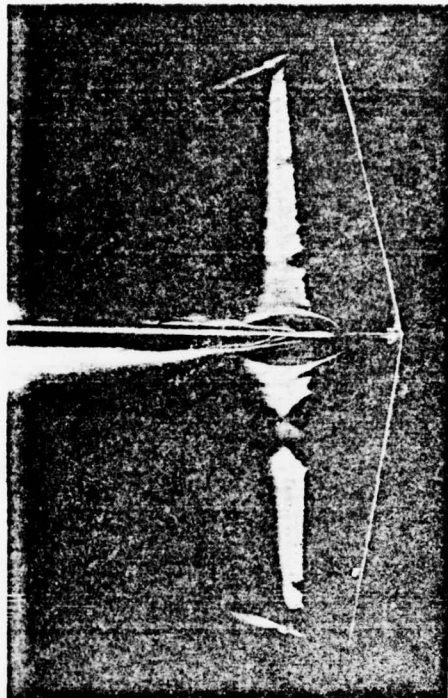
α = 1.814 deg   α = 2.814 deg

Figure 8(c) – V = 50 Knots, d/c' = 1.0
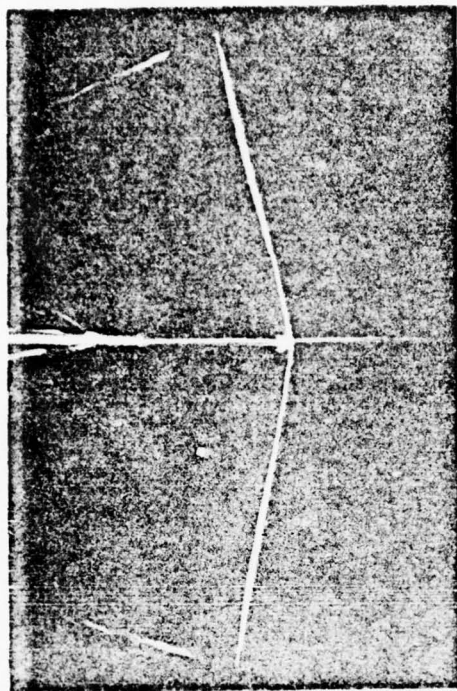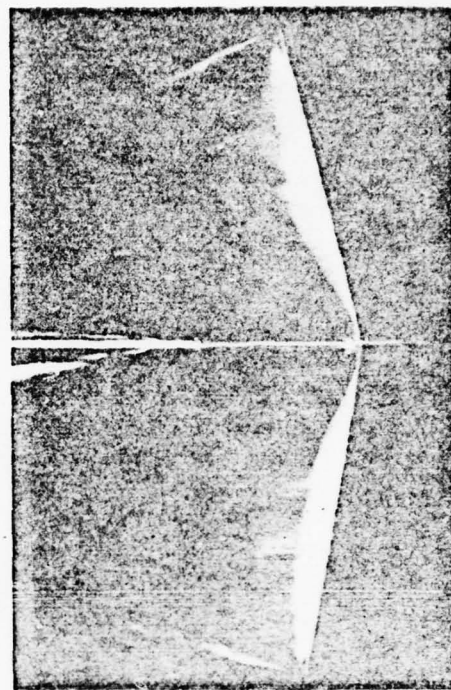
α = 3.814 deg
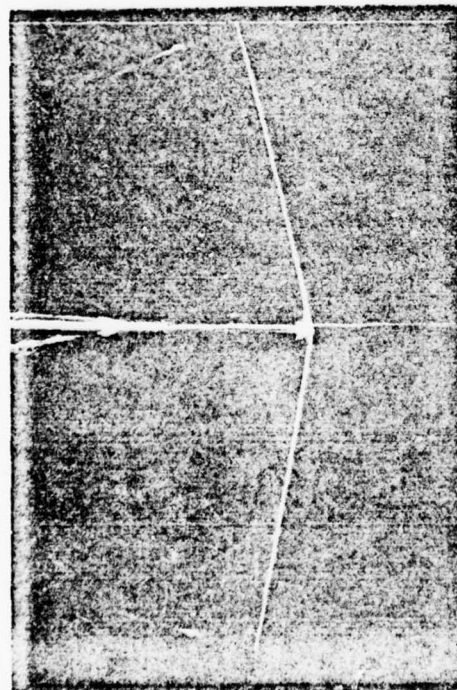
α = 4.814 deg
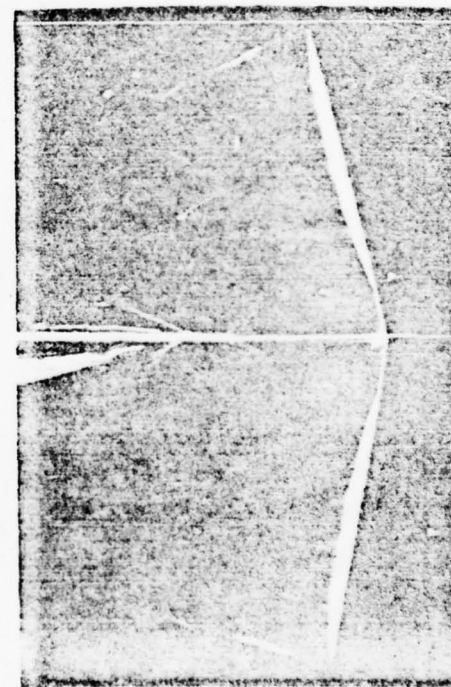
α = 5.814 deg

α = 6.814 deg

Figure 8(d) - V = 30 Knots, d/c' = 2.0

31
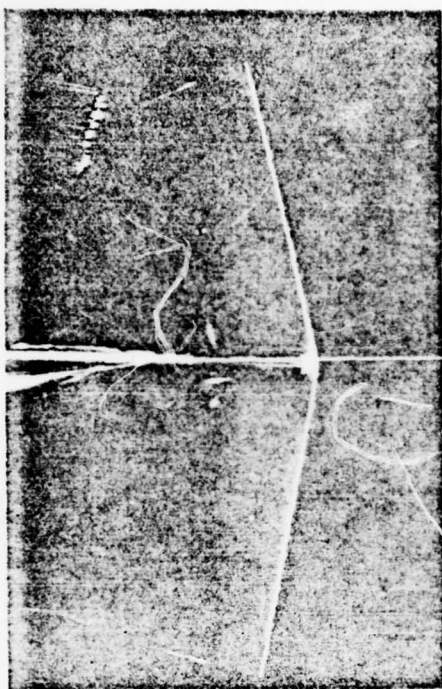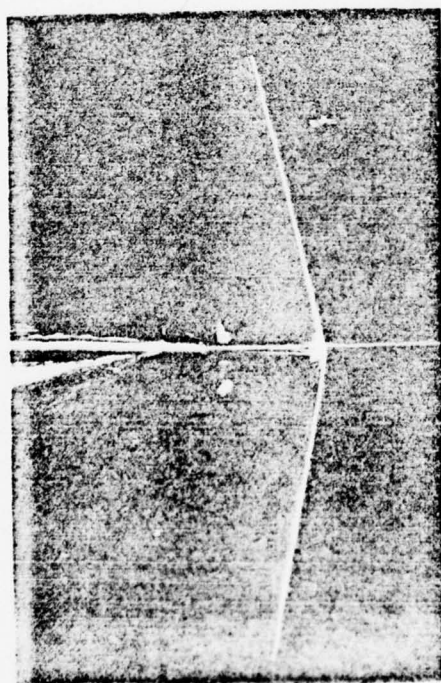
α = -1.186 deg
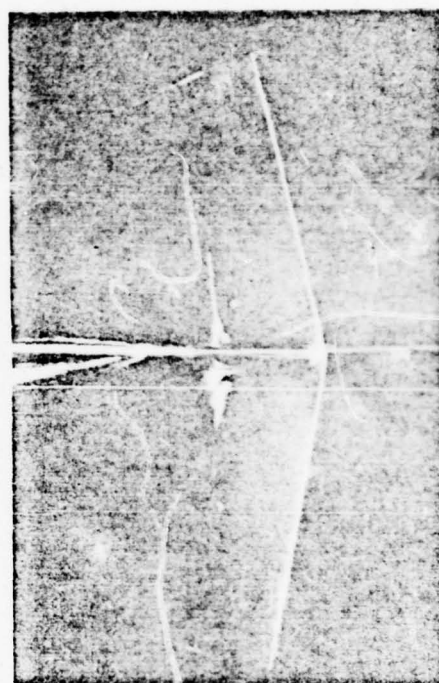
α = -0.186 deg

α = 0.814 deg

Figure 8(e) - V = 35 Knots, d/c' = 2.0

32
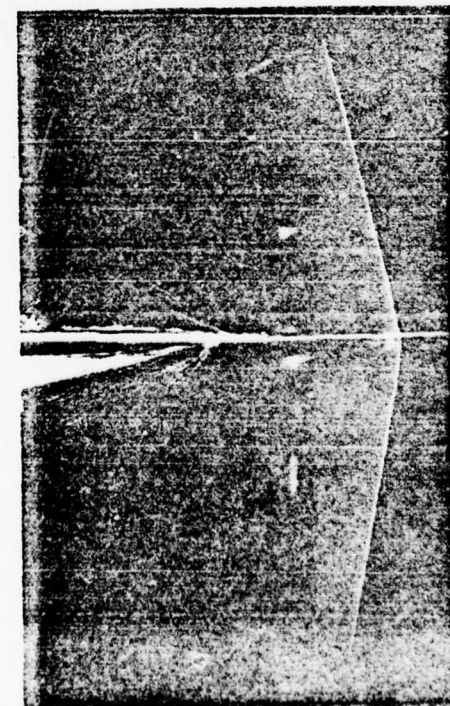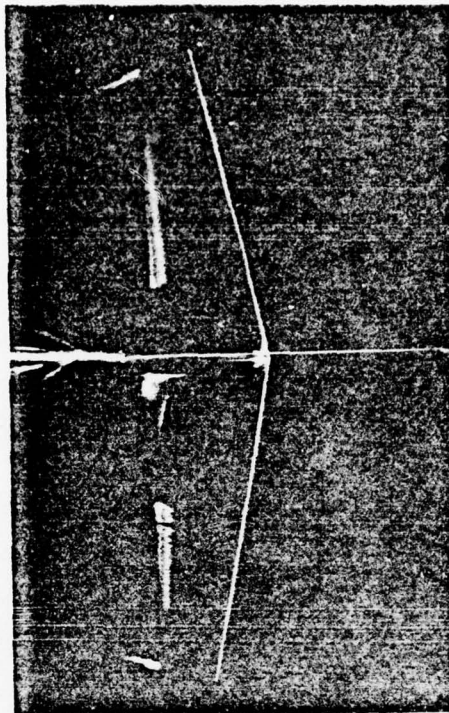
α = 1.814 deg

α = 3.814 deg

Figure 8(f) - V = 35 Knots, d/c' = 2.0

33
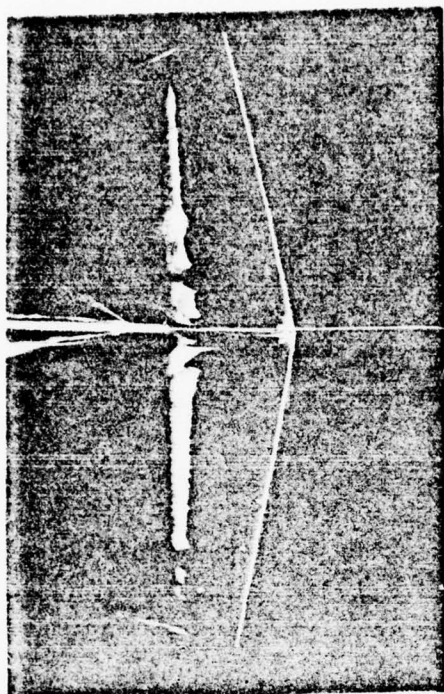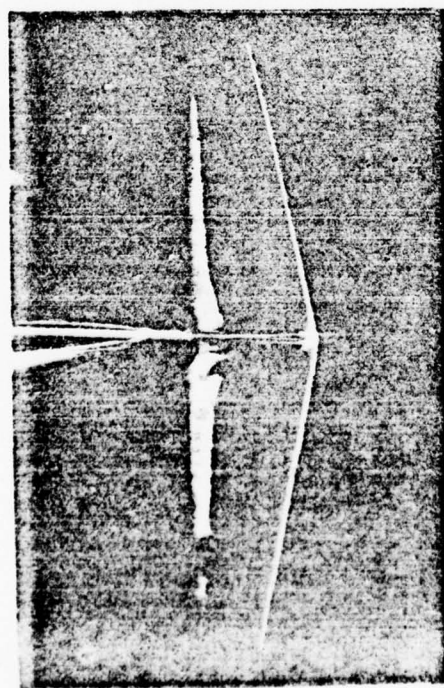
α = -0.186 deg
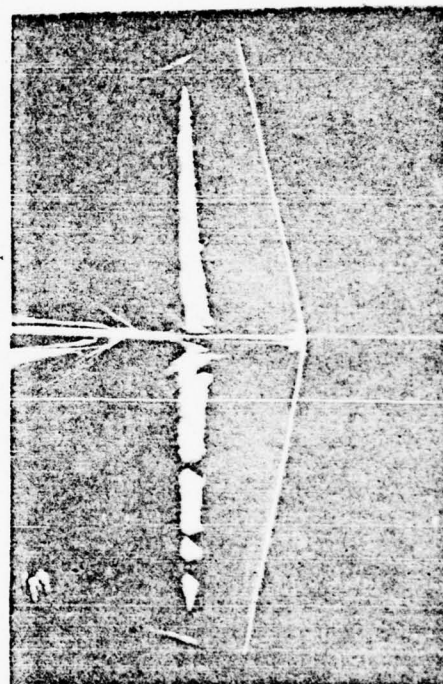
α = -1.186 deg

α = 0.814 deg

Figure 8(g) - V = 40 Knots, d/c' = 2.0

34
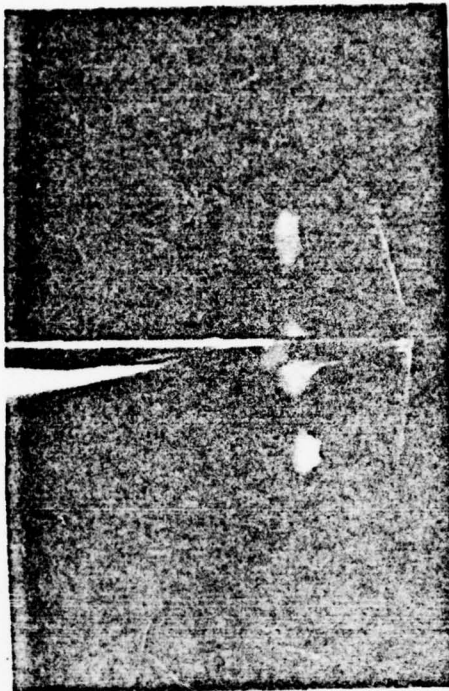
α = 1.814 deg

α = 2.814 deg

Figure 8(h) - V = 40 Knots, d/c' = 2.0

35
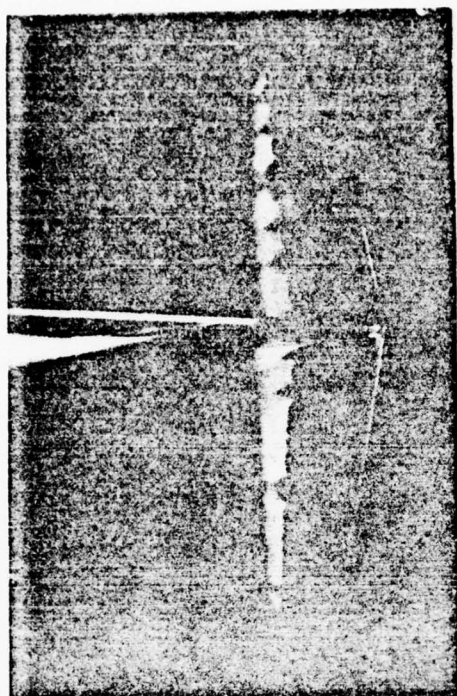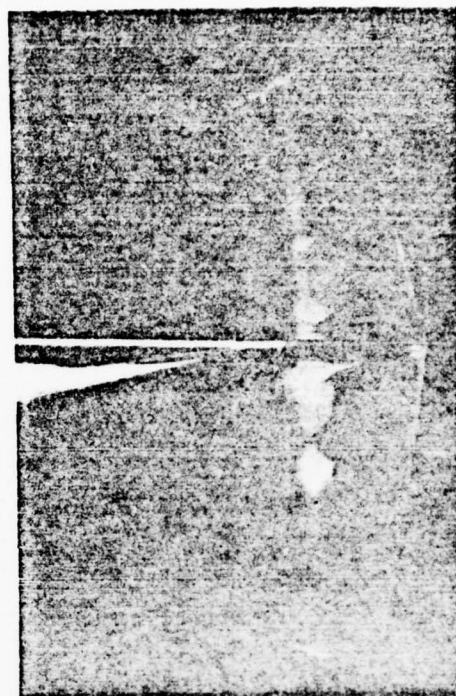
α = 0.814 deg

α = 2.814 deg
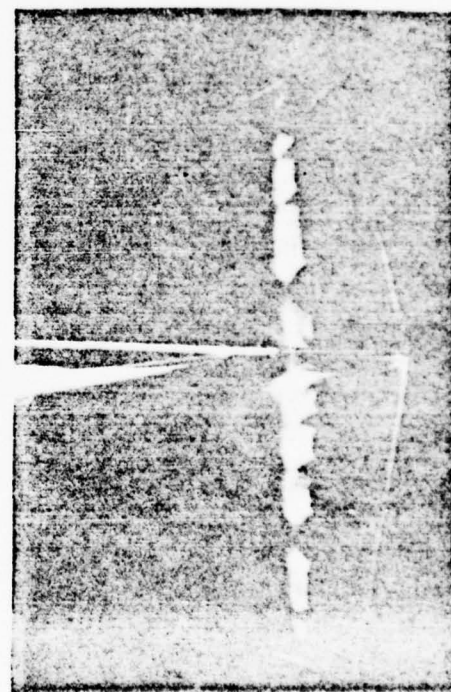
α = -0.186 deg

α = 1.814 deg

Figure 8(i) - V = 45 Knots, d/c' = 2.0

36
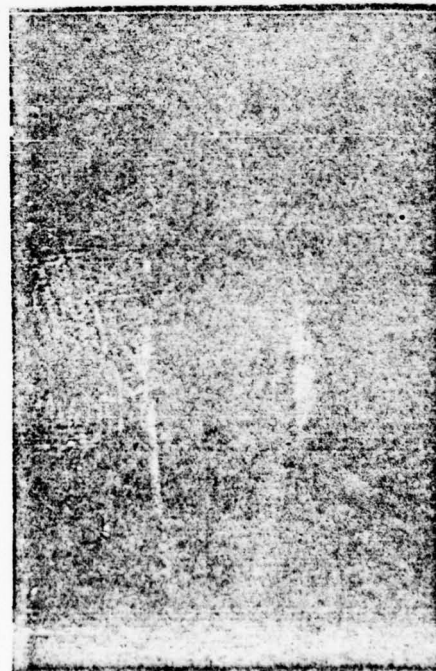
$\alpha = -0.186$ deg
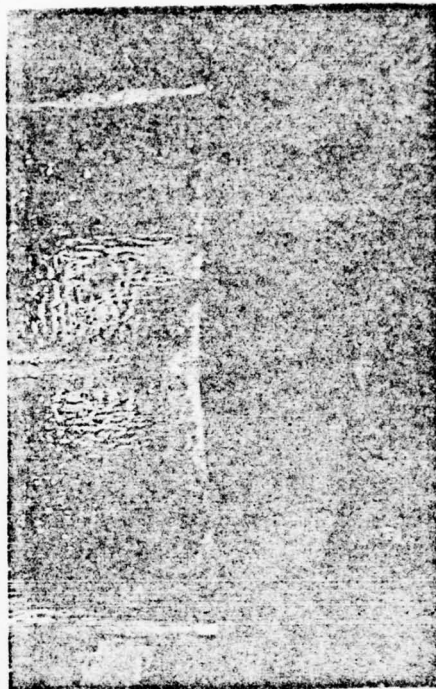
$\alpha = 2.814$ deg

$\alpha = -1.186$ deg

$\alpha = 1.814$ deg

Figure 9(a) – V = 45 Knots, d/c' = 1.0

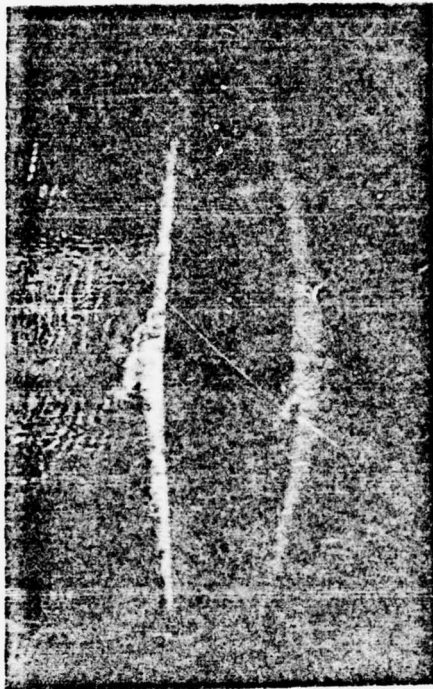Figure 9 – Underwater Photographs of Pressure Side View of TAP-2 Strut-Foil Model at Various Experimental Conditions

α = -0.186 deg

α = 1.814 deg

Figure 9(b) – V = 50 Knots, d/c' = 1.0

38
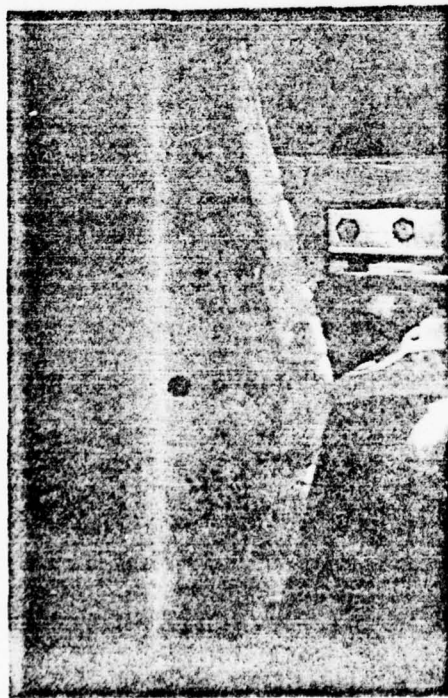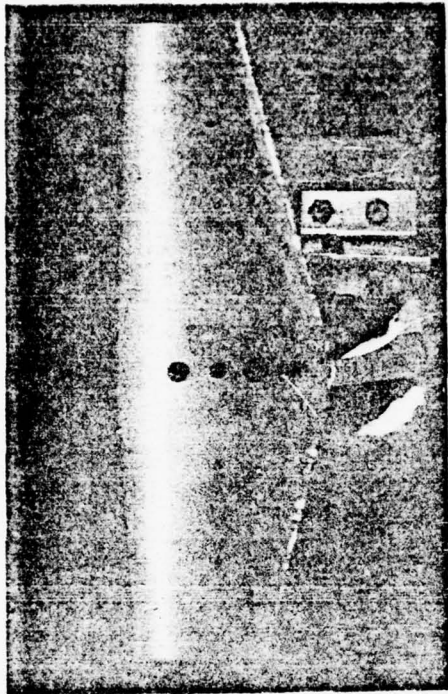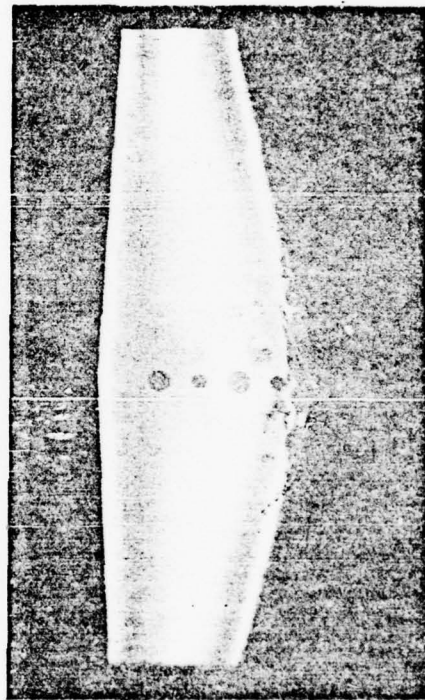
$\alpha = -2.186$ deg

$\alpha = -1.186$ deg

$\alpha = -0.186$ deg

Figure 9(c) – V = 35 Knots, d/c' = 2.0

α = 0.814 deg

α = 1.814 deg

Figure 9(d) – V = 35 Knots, d/c' = 2.0

40

α = -2.186 deg
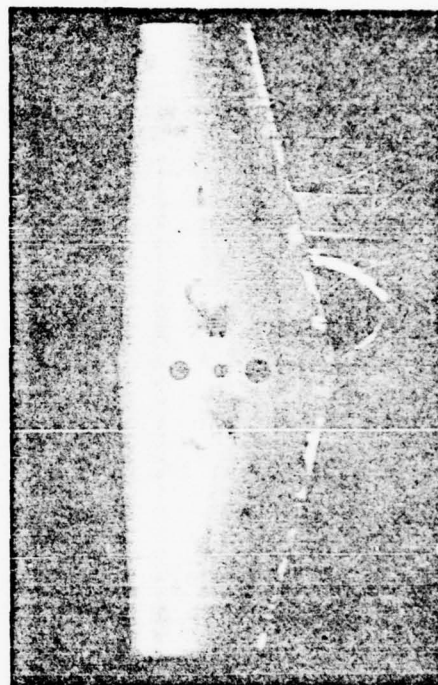
α = -1.186 deg

α = -0.186 deg

Figure 9(e) - V = 40 Knots, d/c' = 2.0

41

α = 1.814 deg

α = 0.814 deg

α = 2.814 deg

Figure 9(f) - V = 40 Knots, d/c' = 2.0

42
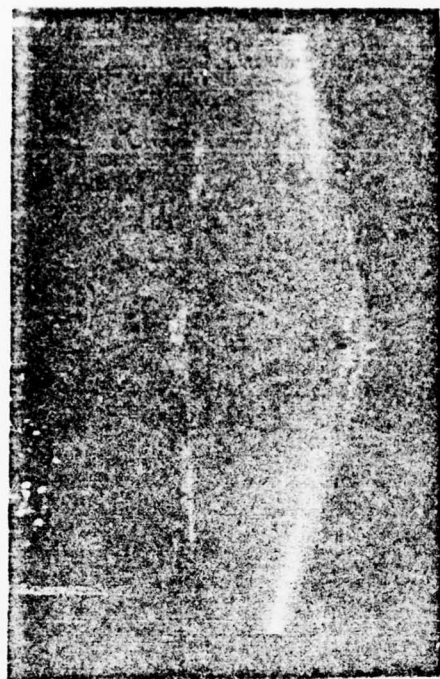
α = 0.814 deg
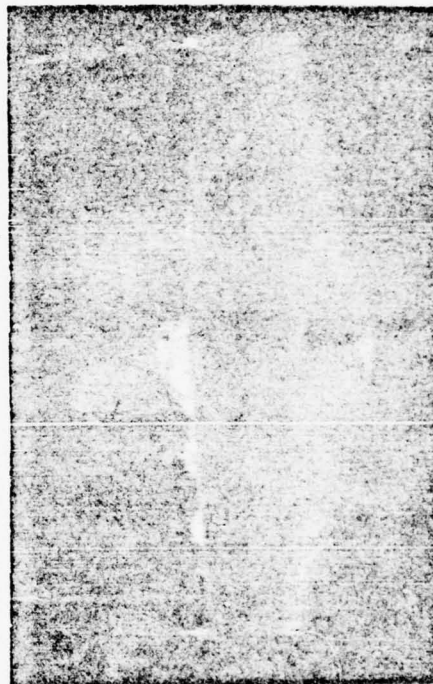
α = 1.814 deg

α = 2.814 deg

Figure 9(g) - V = 45 Knots, d/c' = 2.0

43

α = -0.186 deg

α = 1.814 deg

α = -1.186 deg
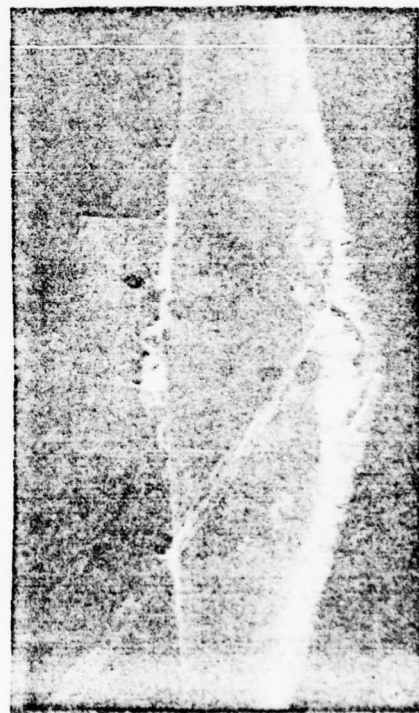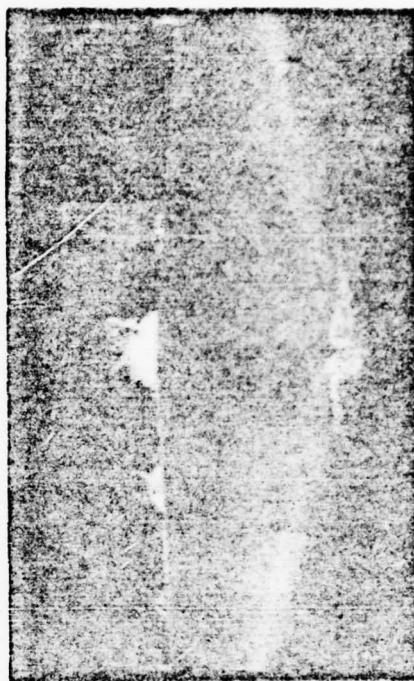
α = 0.814 deg

Figure 9(h) - V = 45 Knots, d/c' = 3.0

44
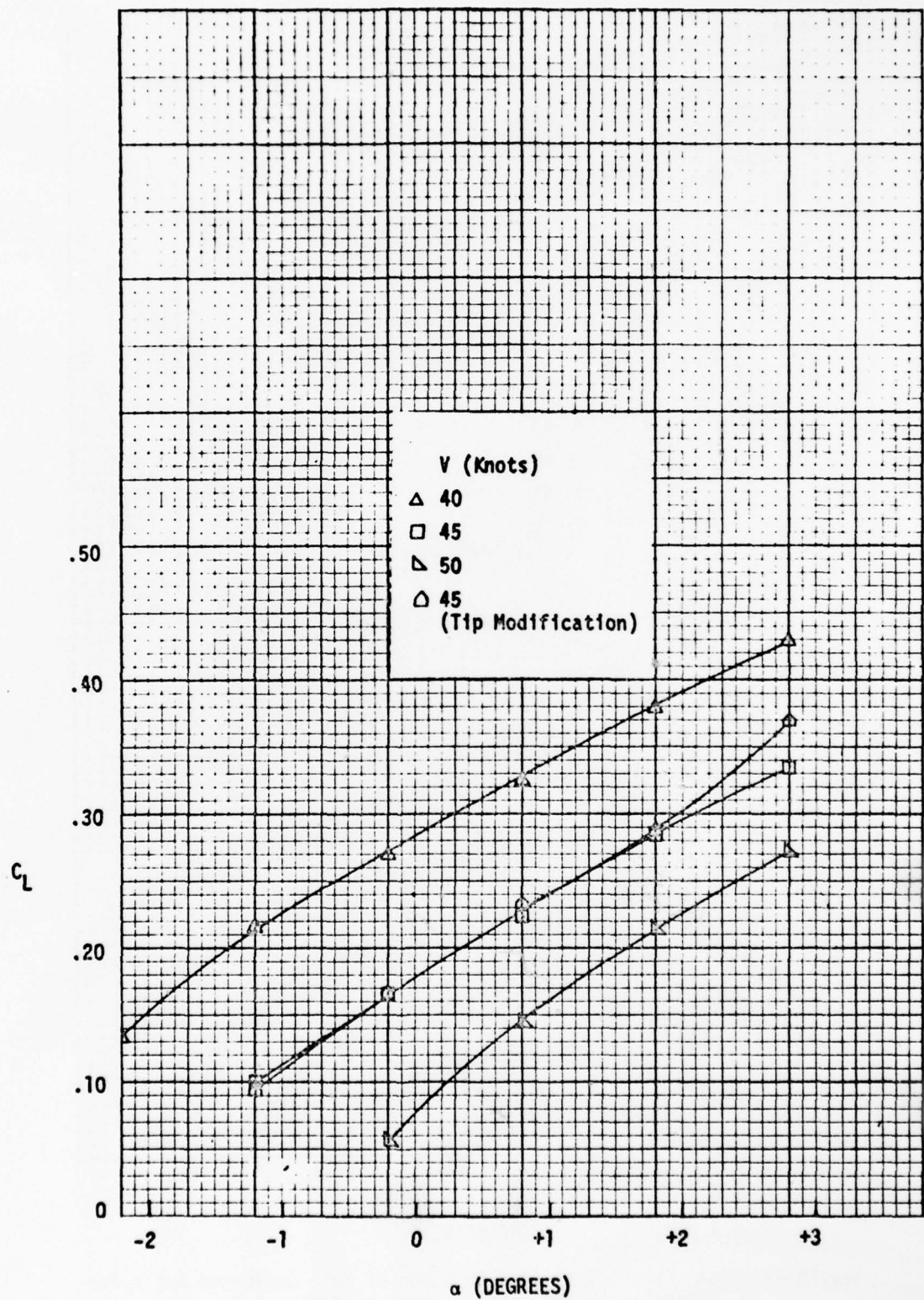
Figure 10 - Lift Coefficient as a Function of Foil Incidence Angle for
Speeds of 40, 45, and 50 Knots at d/c' = 1.0

45
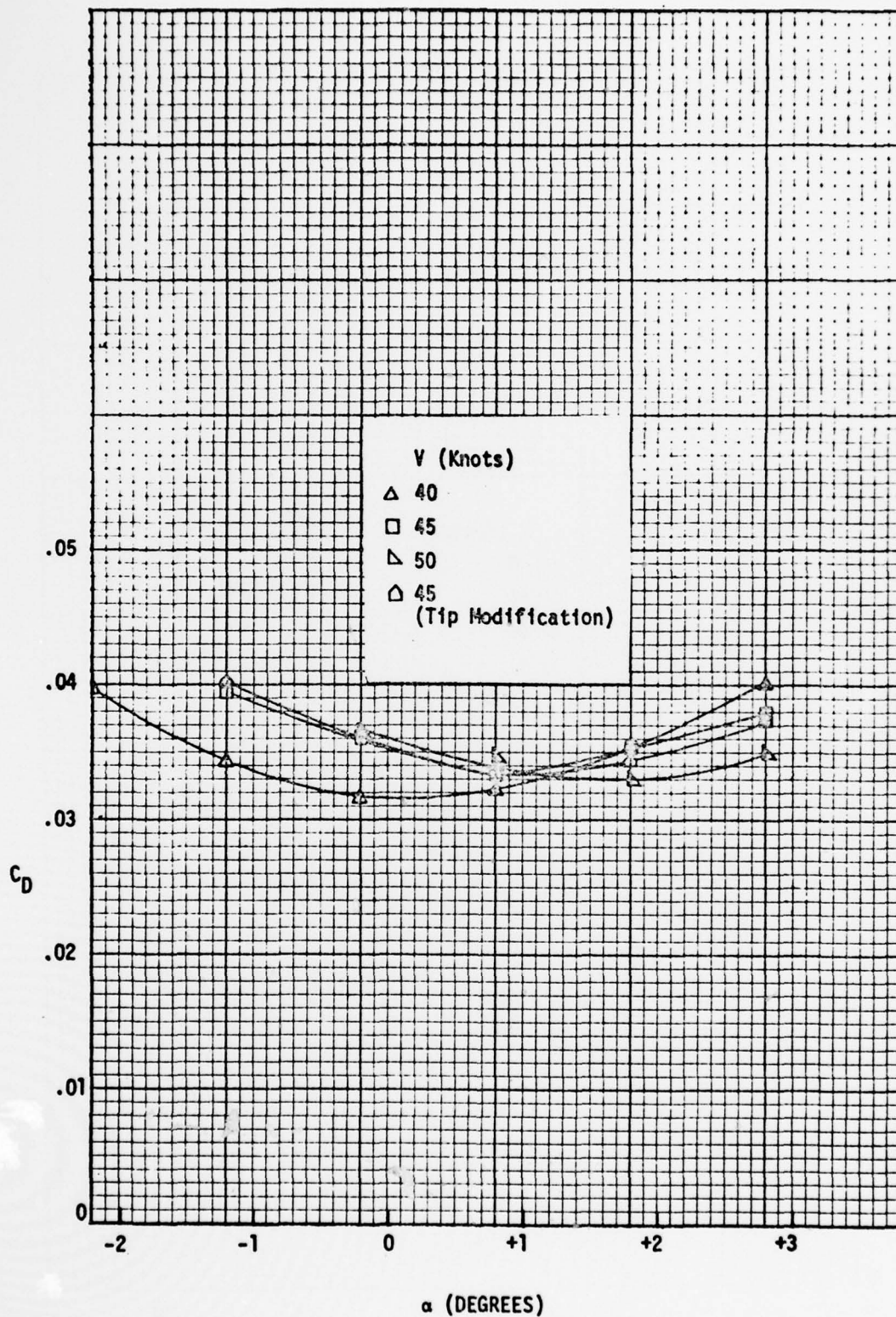
Figure 11 - Drag Coefficient as a Function of Foil Incidence Angle for Speeds of 40, 45, and 50 Knots at d/c' = 1.0

46
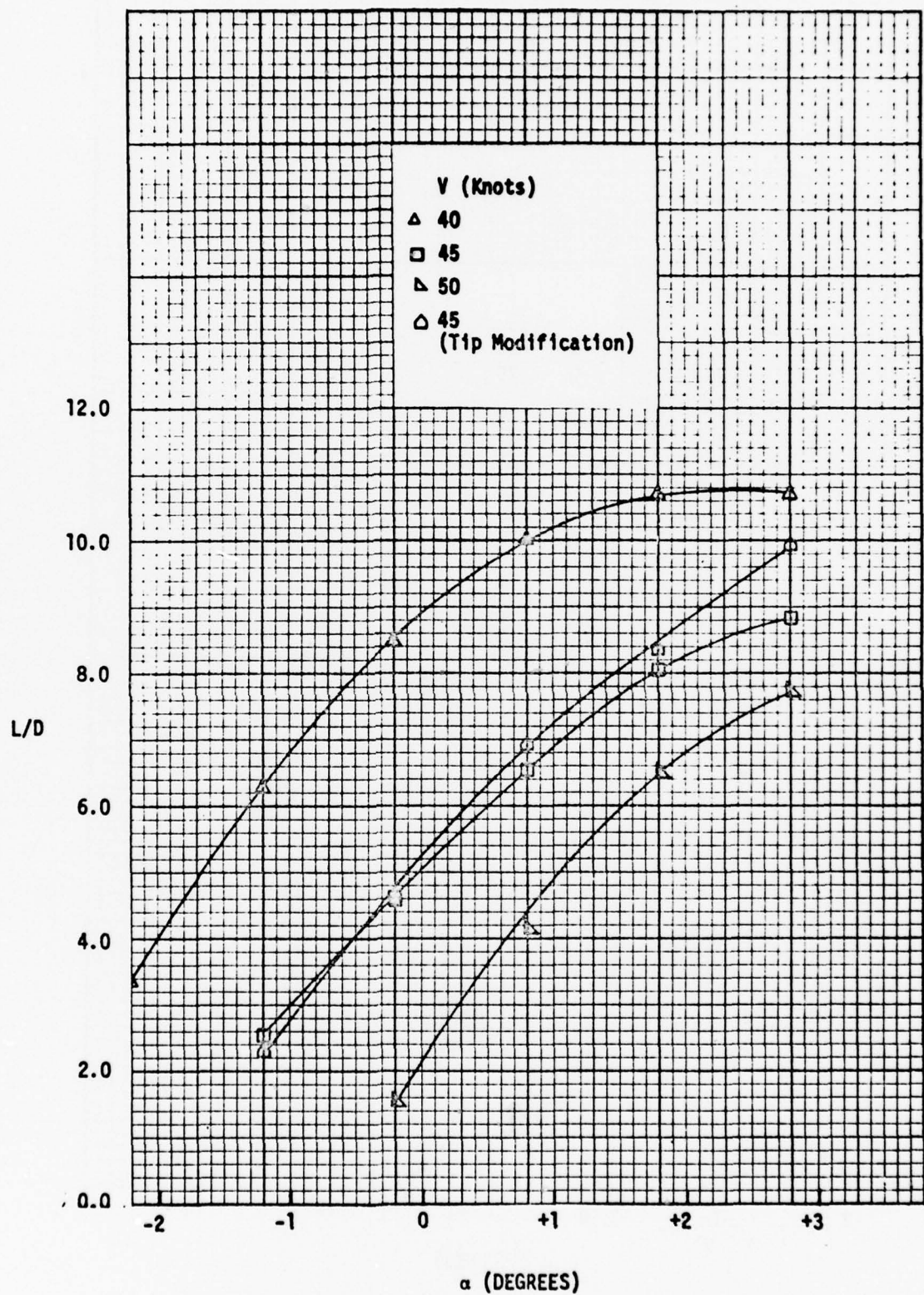
Figure 12 - Lift-to-Drag Ratio as a Function of Foil Incidence Angle
at Speeds of 40, 45, and 50 Knots at d/c' = 1.0

47
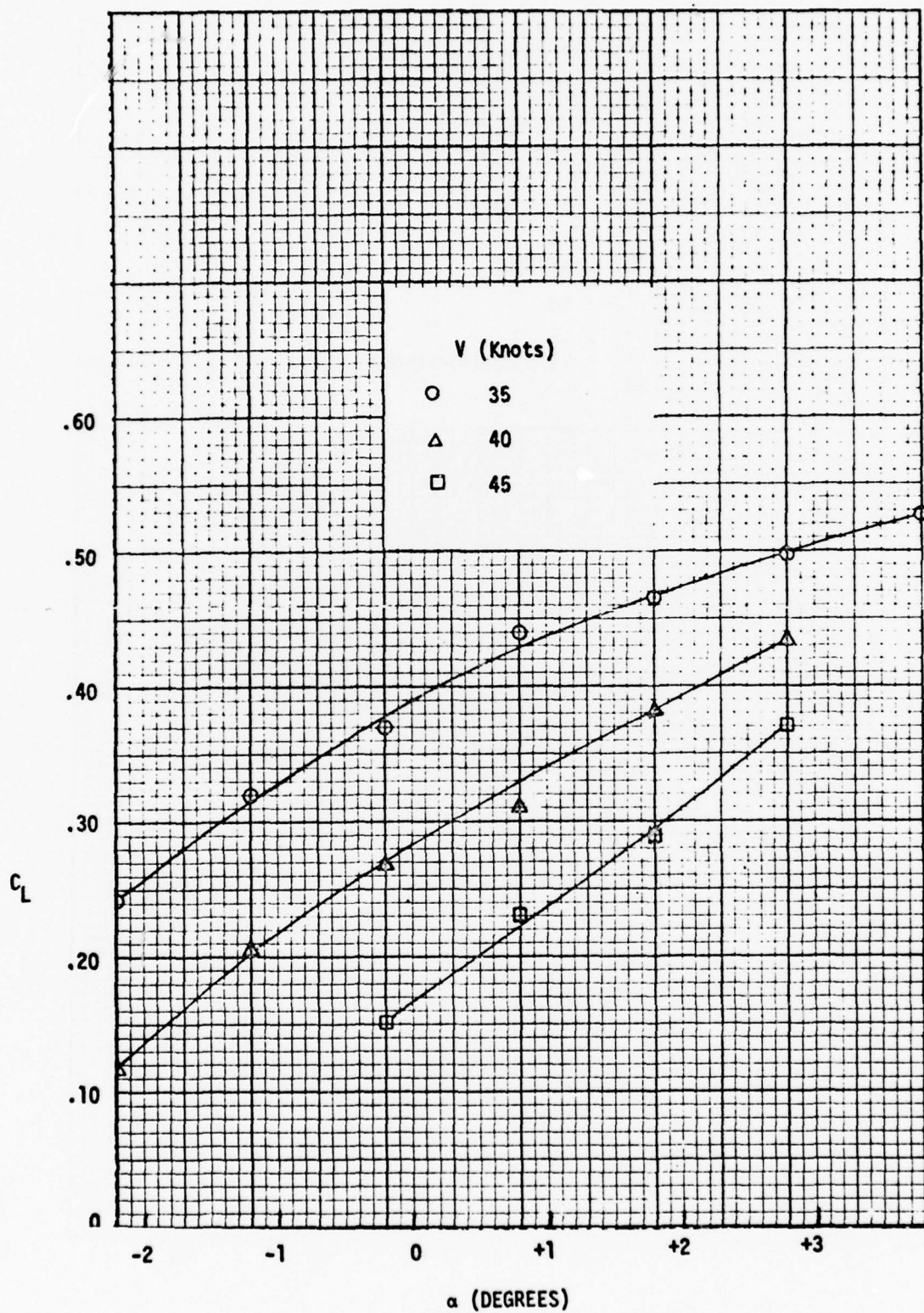
Figure 13 - Lift Coefficient as a Function of Foil Incidence Angle for
Speeds of 35, 40, and 45 Knots at d/c' = 2.0

48
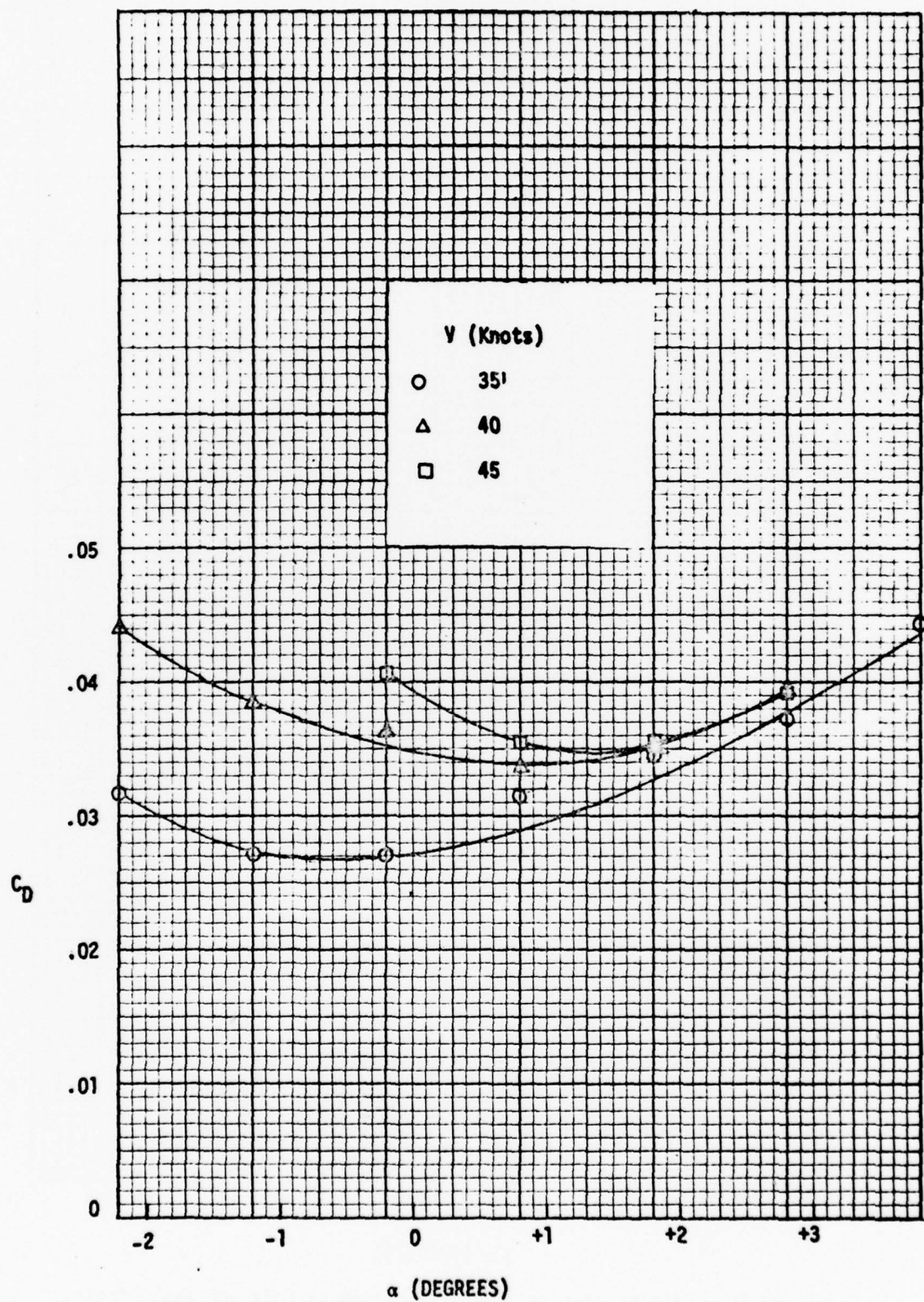
Figure 14 - Drag Coefficient as a Function of Foil Incidence Angle for
Speeds of 35, 40, and 45 Knots at d/c' = 2.0
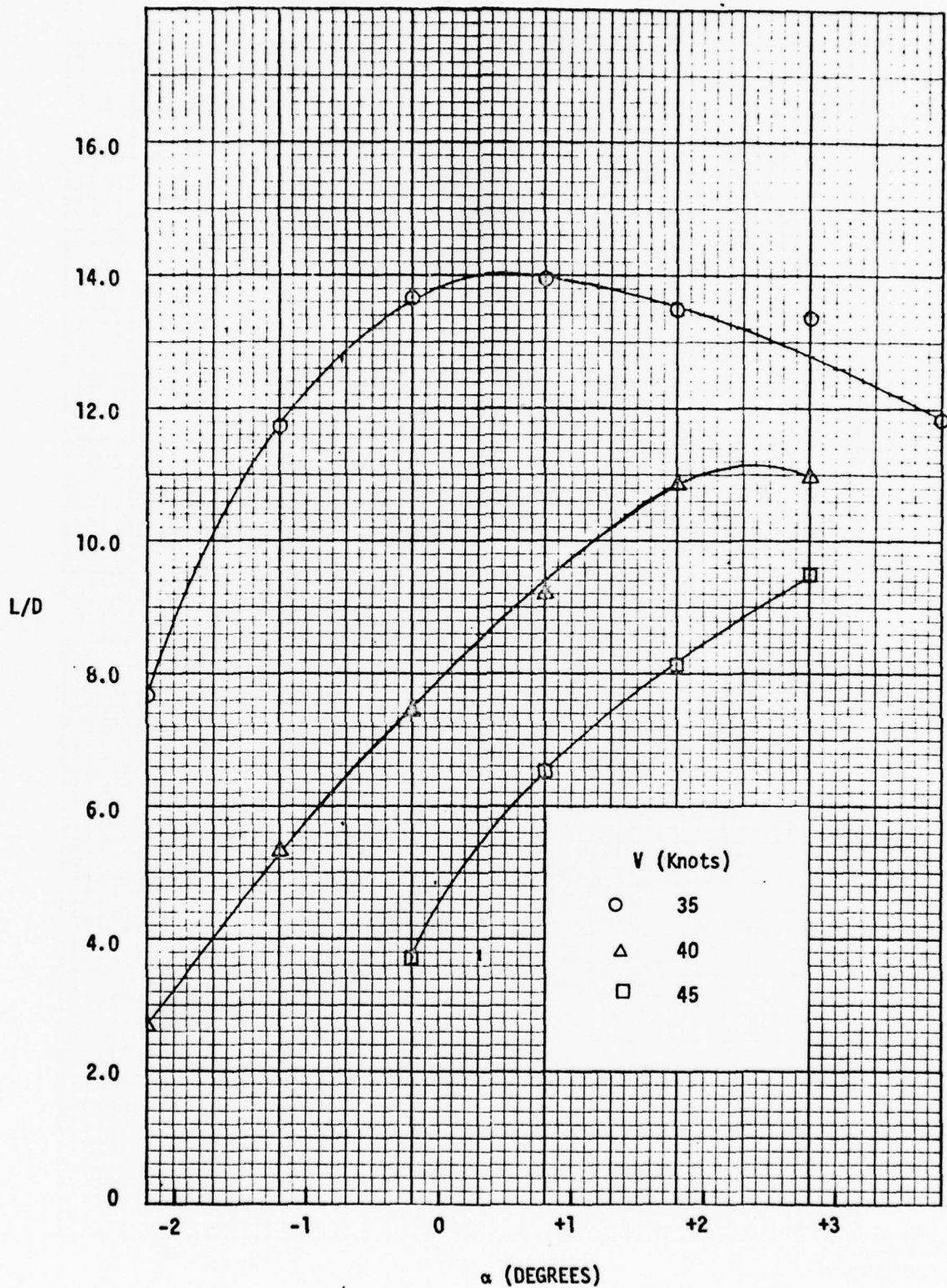
Figure 15 - Lift-to-Drag Ratio as a Function of Foil Incidence Angle at Speeds of 35, 40, and 45 Knots at d/c' = 2.0
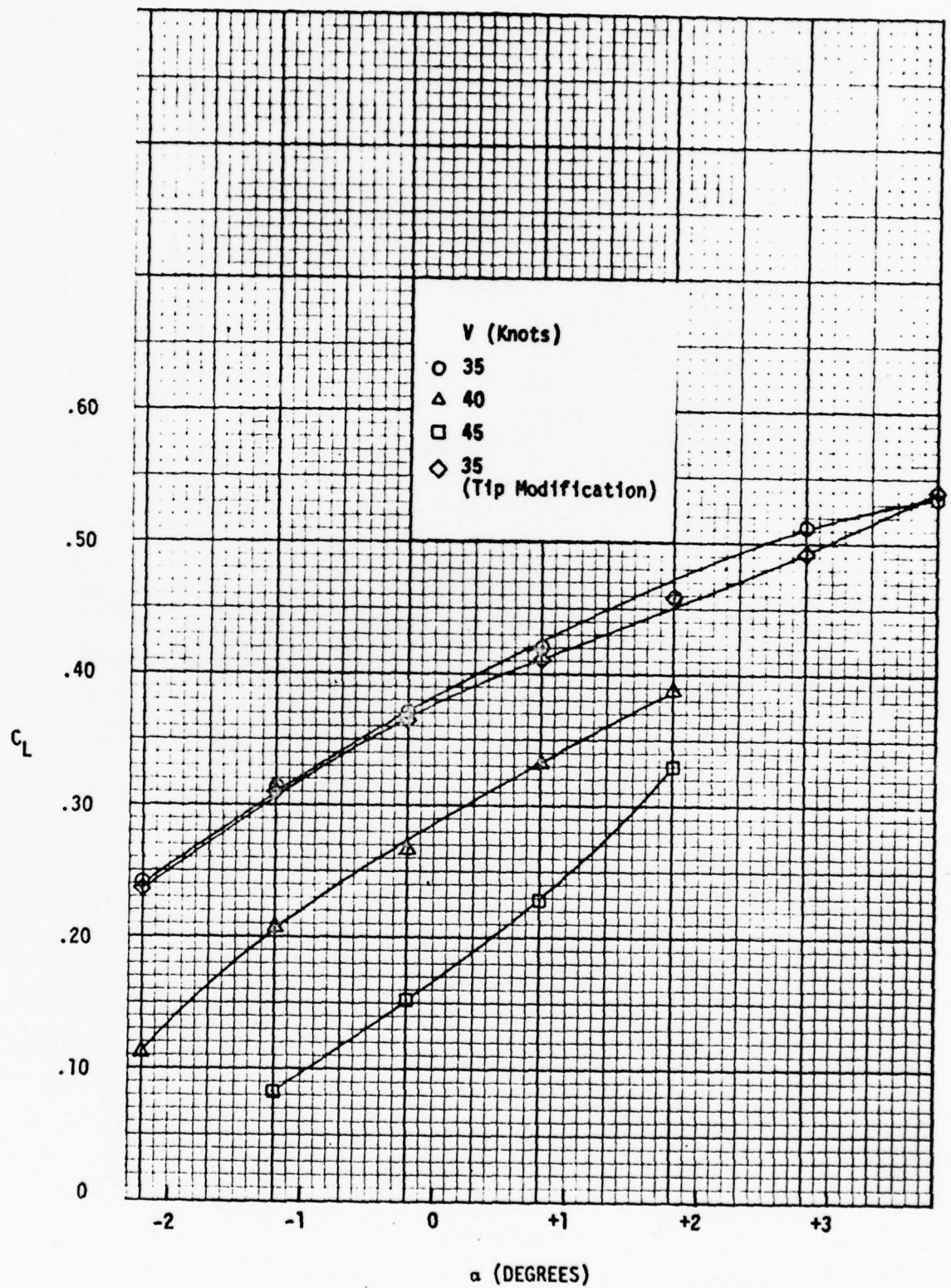
Figure 16 - Lift Coefficient as a Function of Foil Incidence Angle for
Speeds of 35, 40, and 45 Knots at d/c' = 3.0
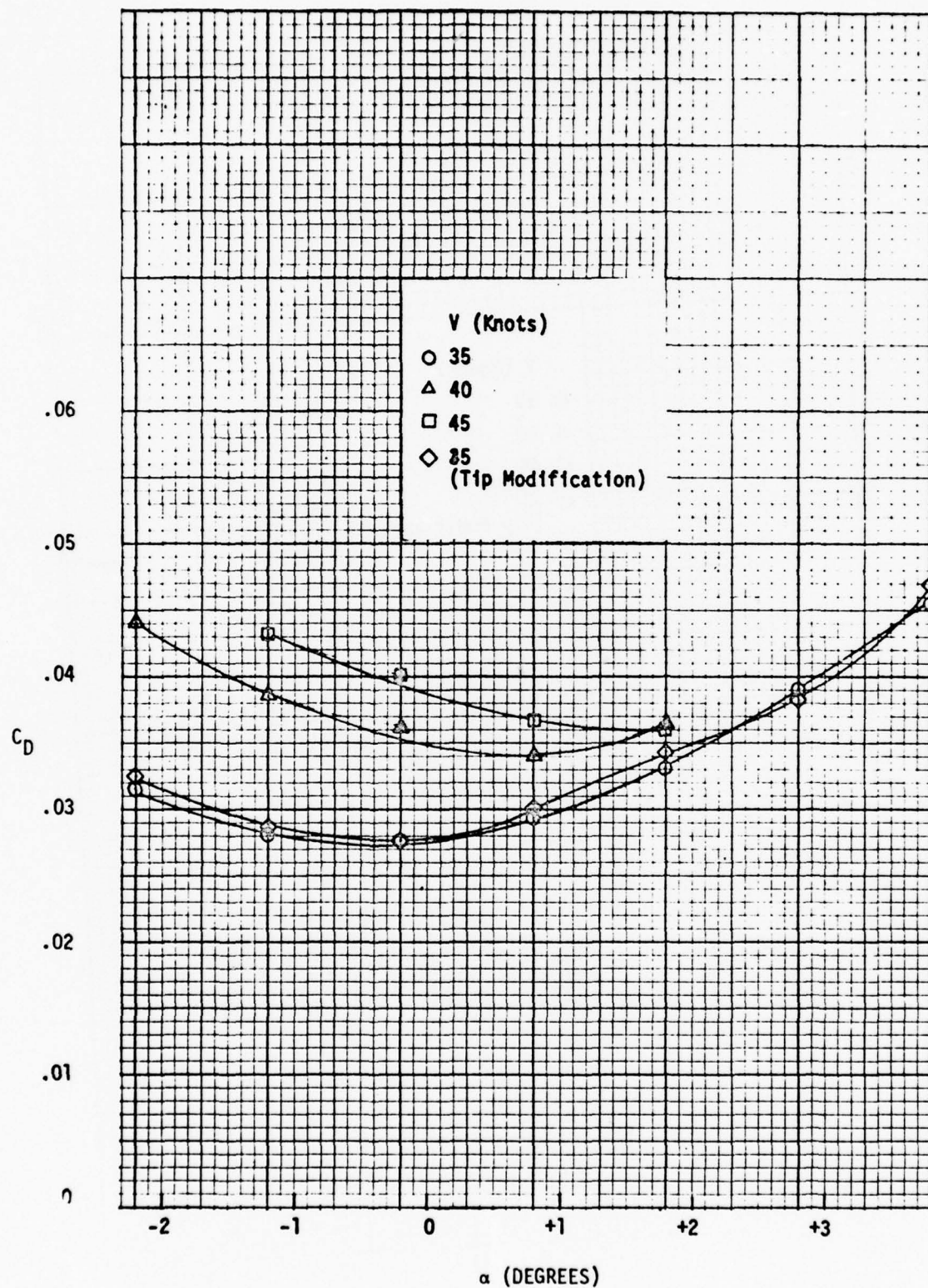
Figure 17 - Drag Coefficient as a Function of Foil Incidence Angle for
Speeds of 35, 40, and 45 Knots at d/c' = 3.0
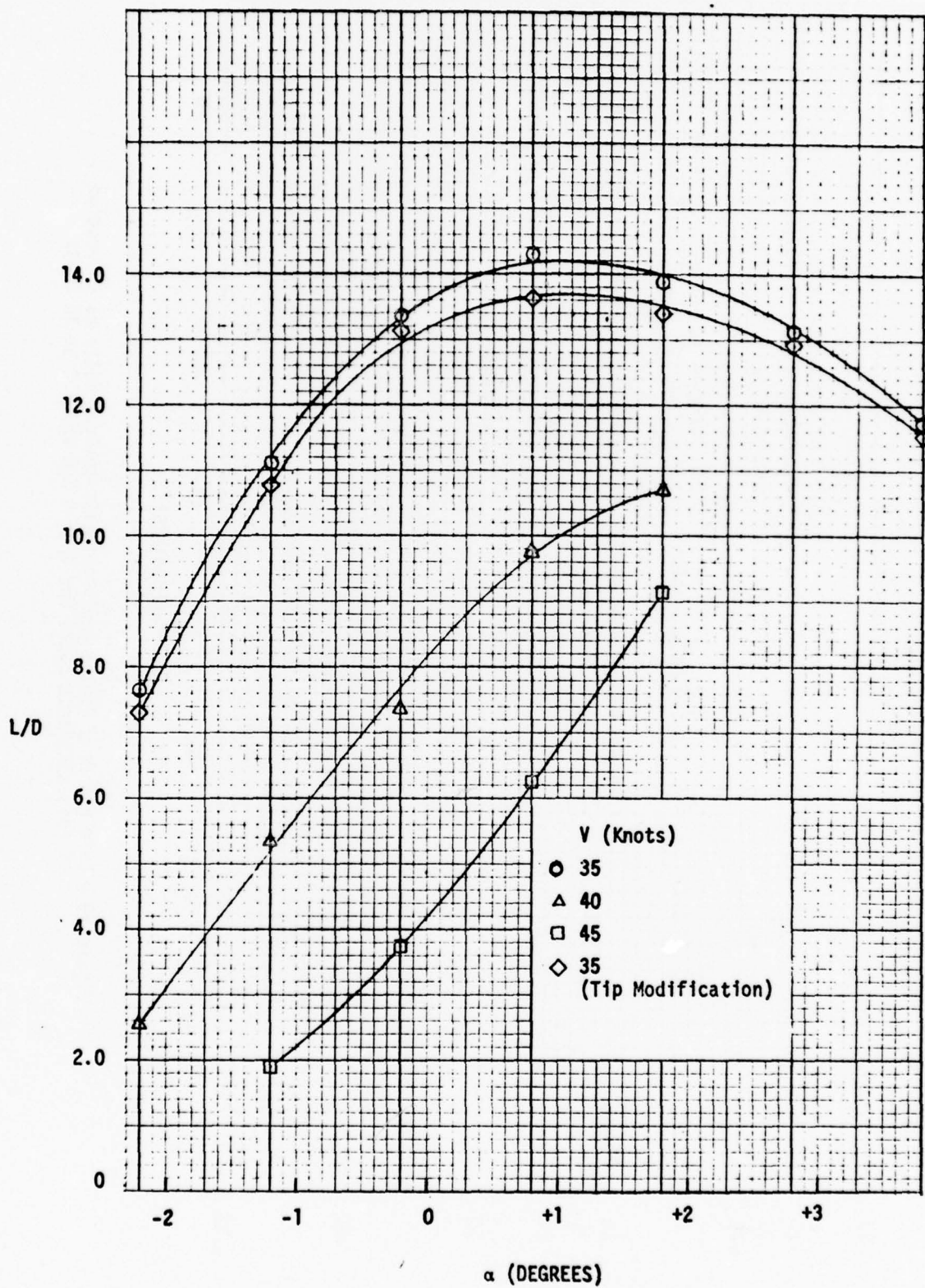
Figure 18 - Lift-to-Drag Ratio as a Function of Foil Incidence Angle
for Speeds of 35, 40, and 45 Knots at d/c' = 3.0

53
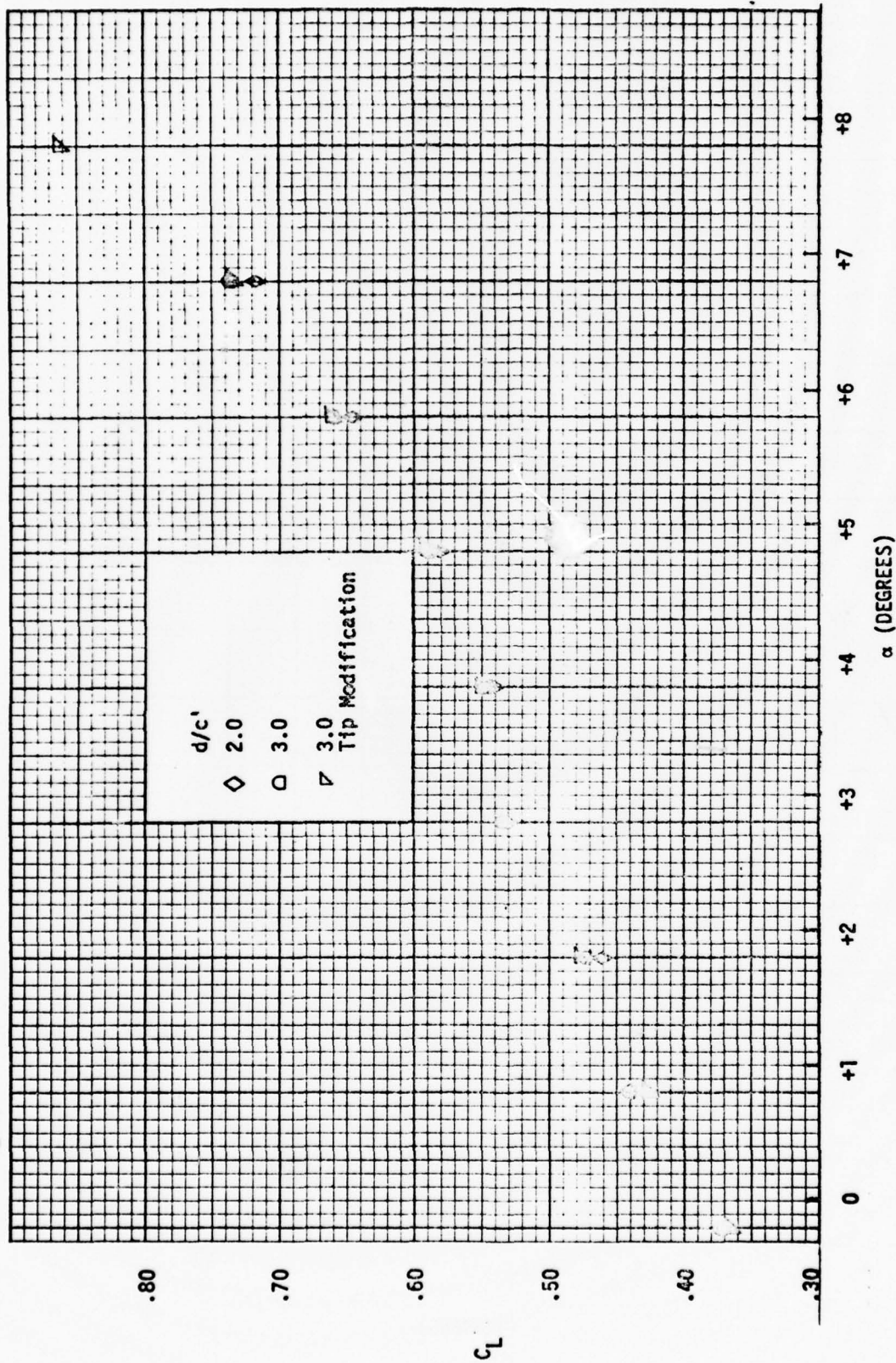
Figure 19 - Lift and Drag Coefficients and Lift-to-Drag Ratio as a Function of Foil Incidence Angle for d/c' = 2.0 and 3.0 at 30 Knots

54

α (DEGREES)

C_D
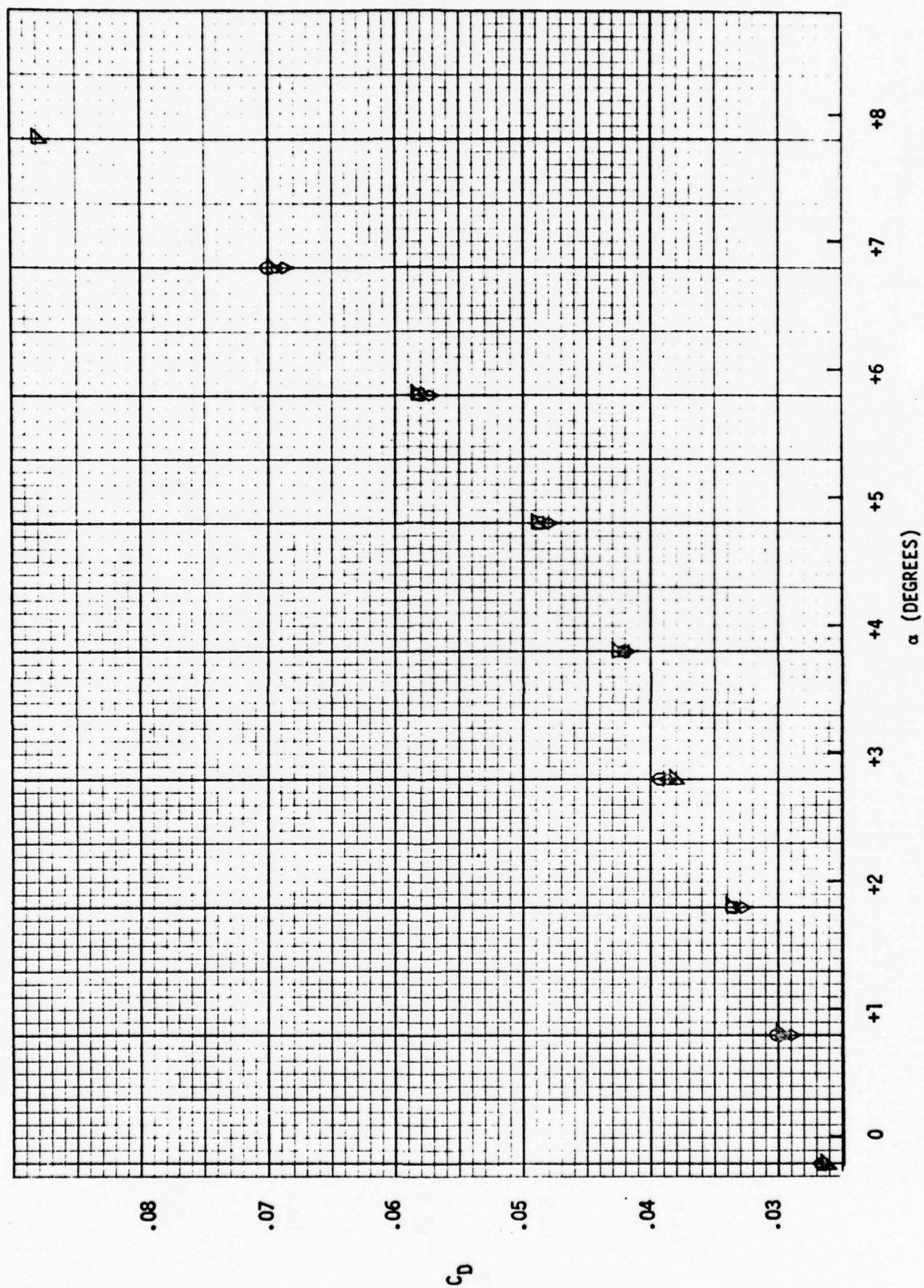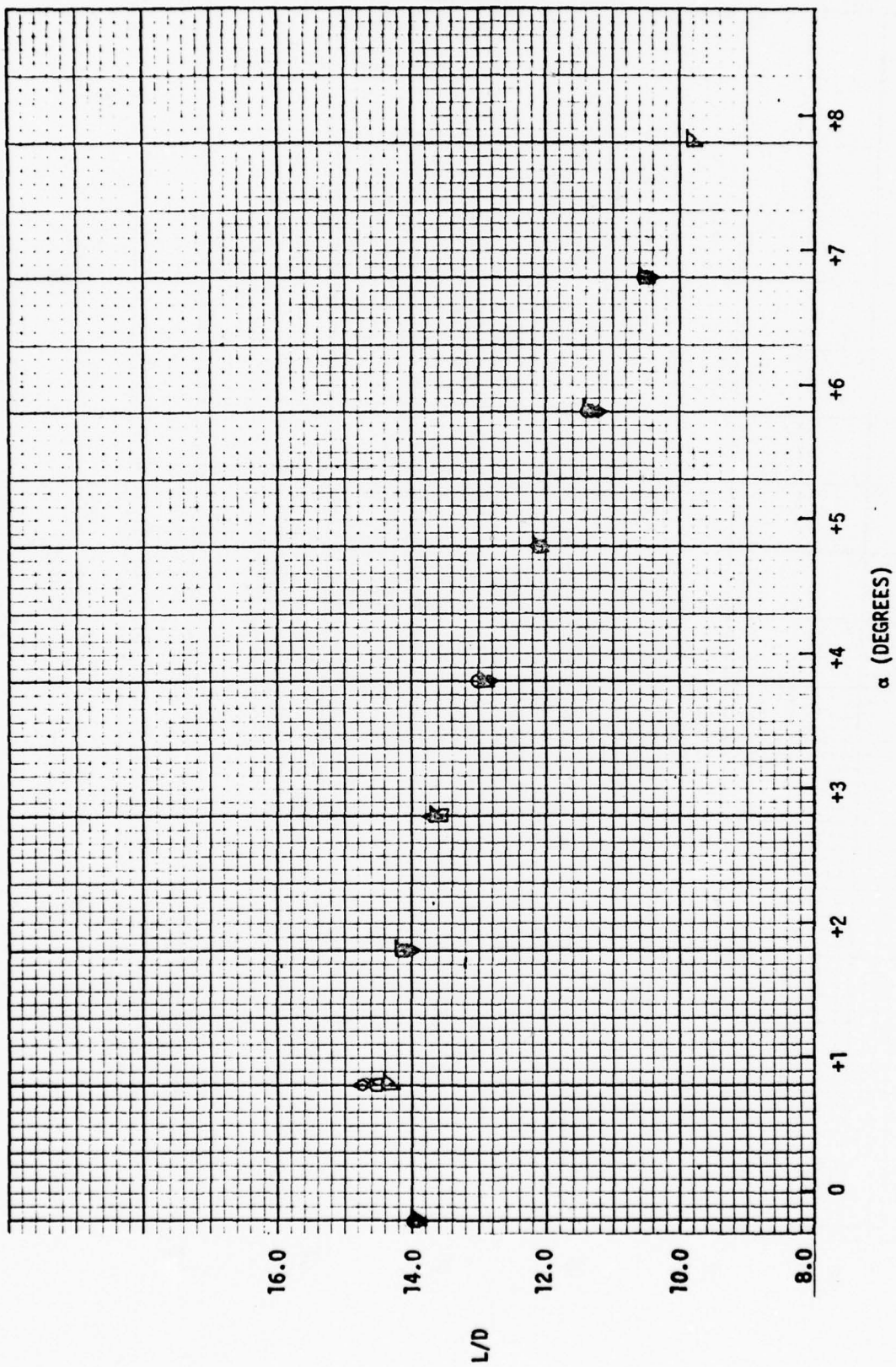
Figure 19 - Continued

Figure 19 – Continued

56
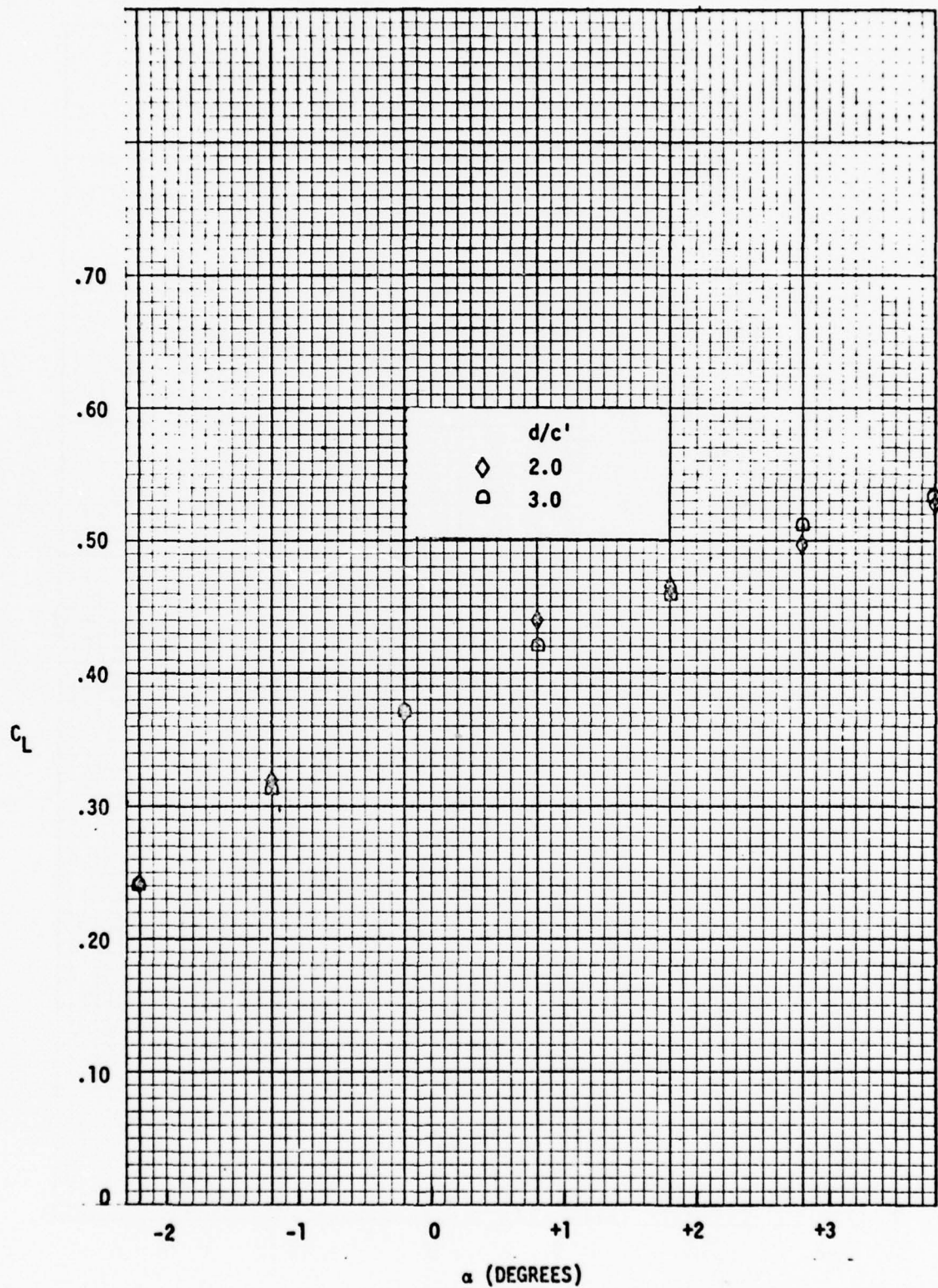
Figure 20 – Lift and Drag Coefficients as a Function of Foil Incidence Angle at 35 Knots for Various Depth-to-Chord Ratios

57
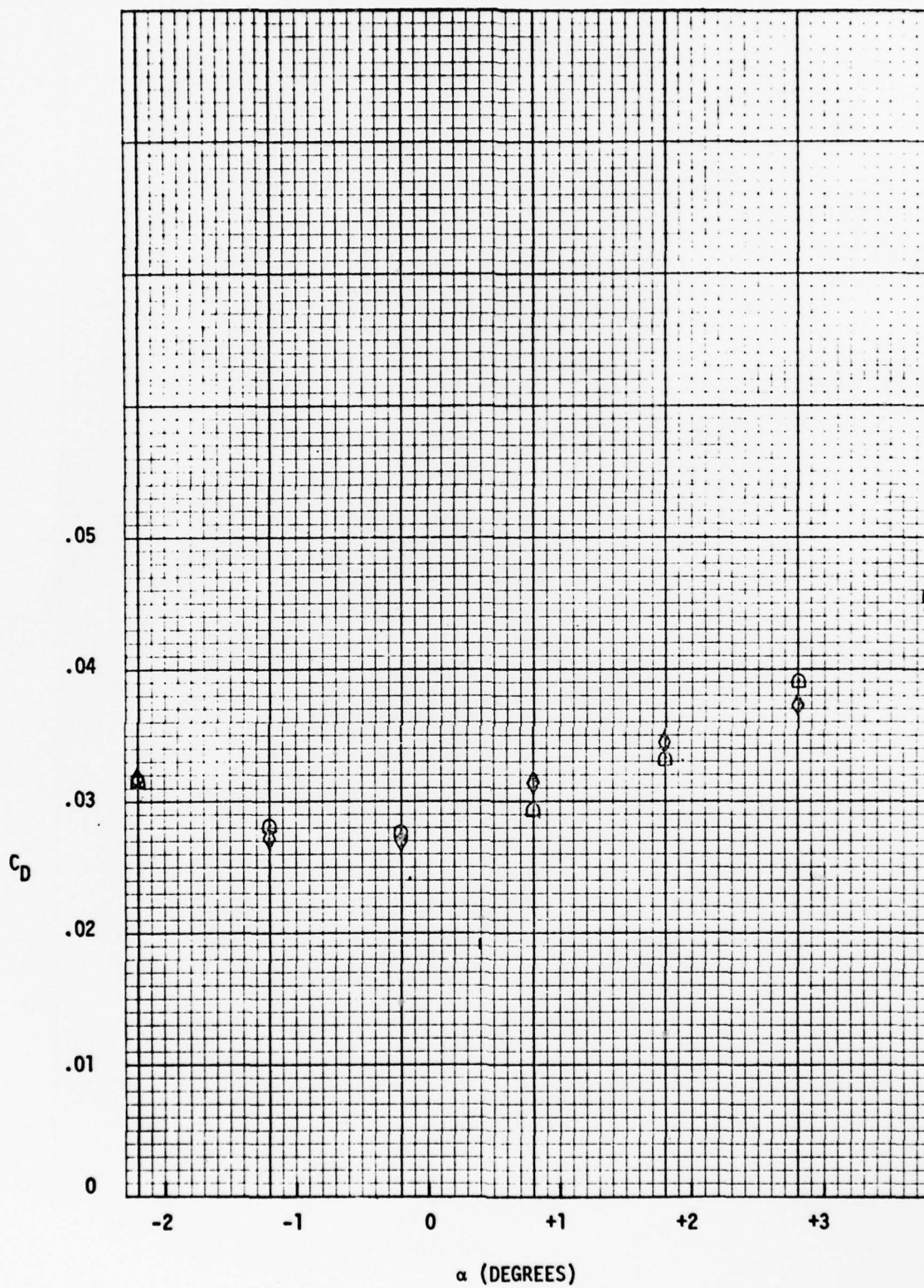
Figure 20 - Continued

58
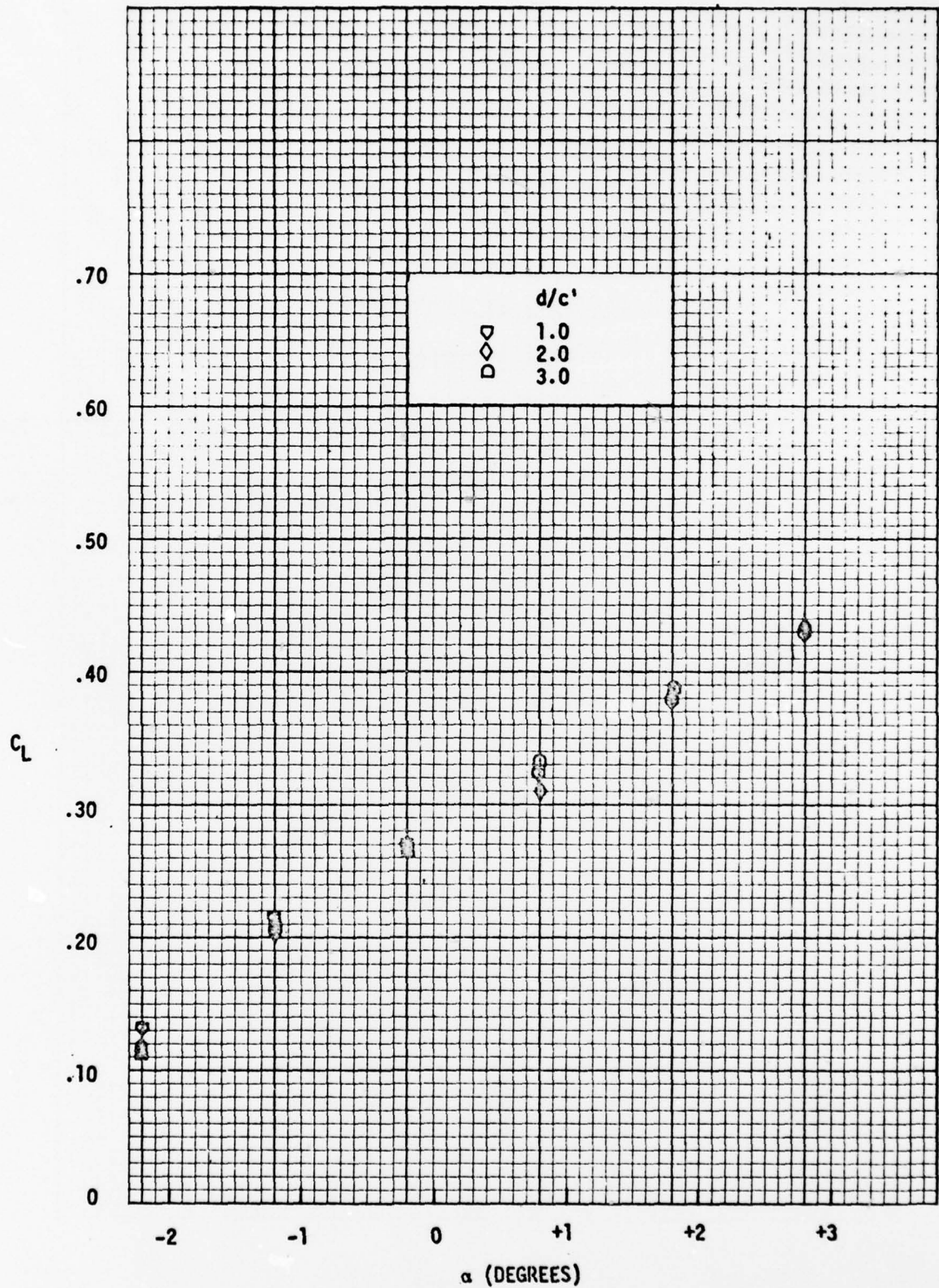
Figure 21 - Lift and Drag Coefficients as a Function of Foil Incidence Angle
at 40 Knots for Various Depth-to-Chord Ratios

59
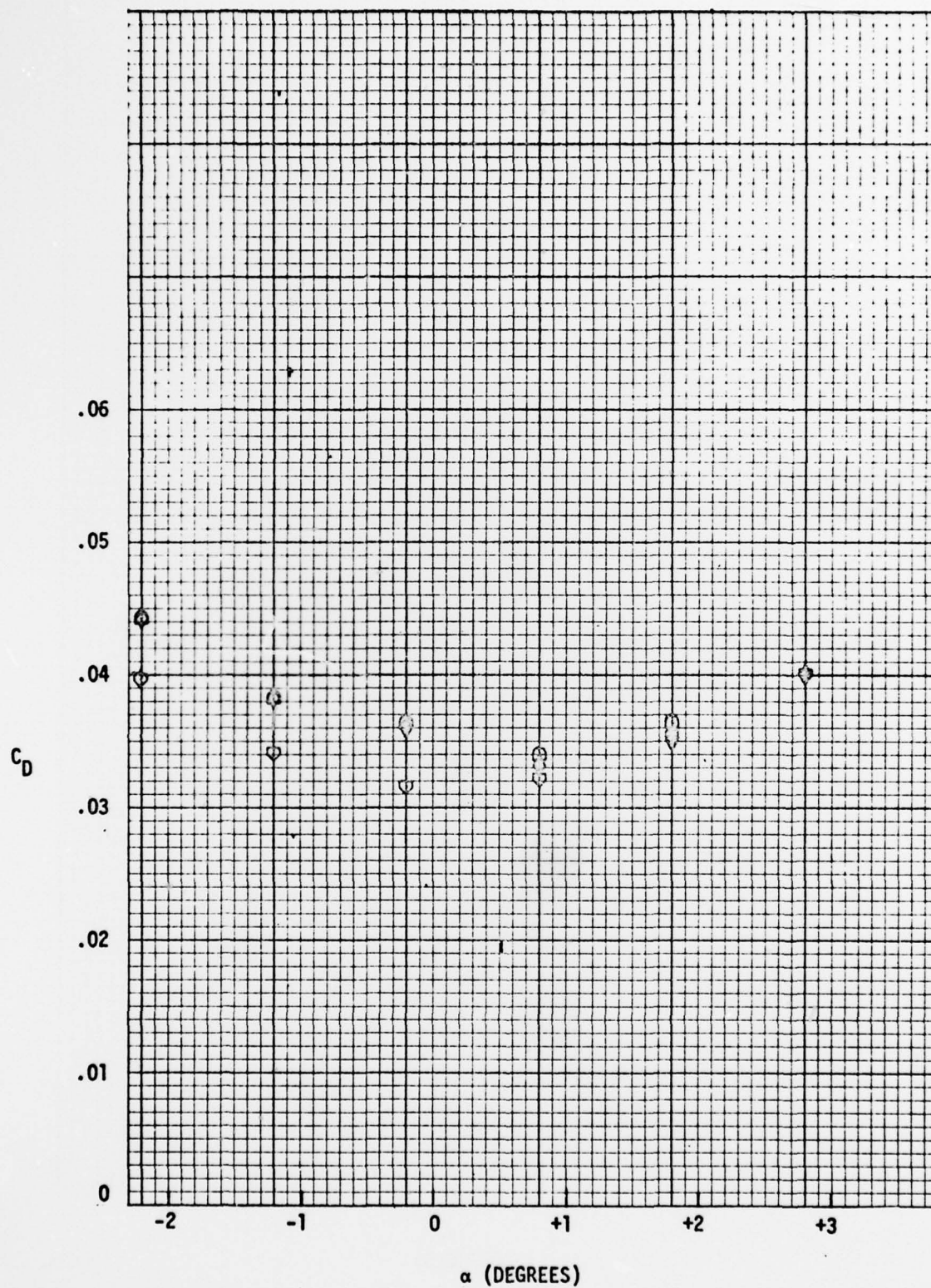
Figure 21 - Continued

60
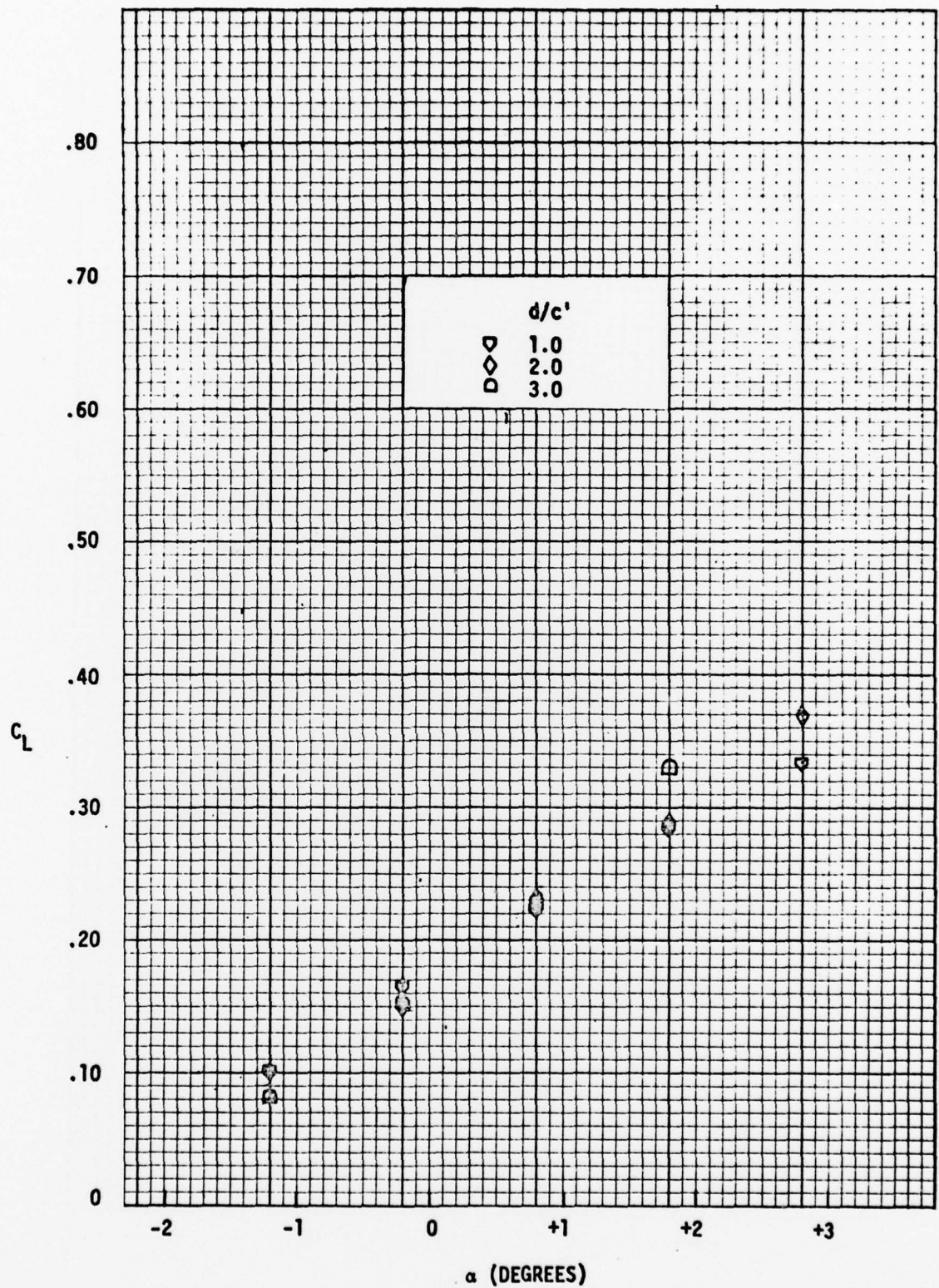
Figure 22 - Lift and Drag Coefficients as a Function of Foil Incidence Angle
at 45 Knots for Various Depth-to-Chord Ratios

61
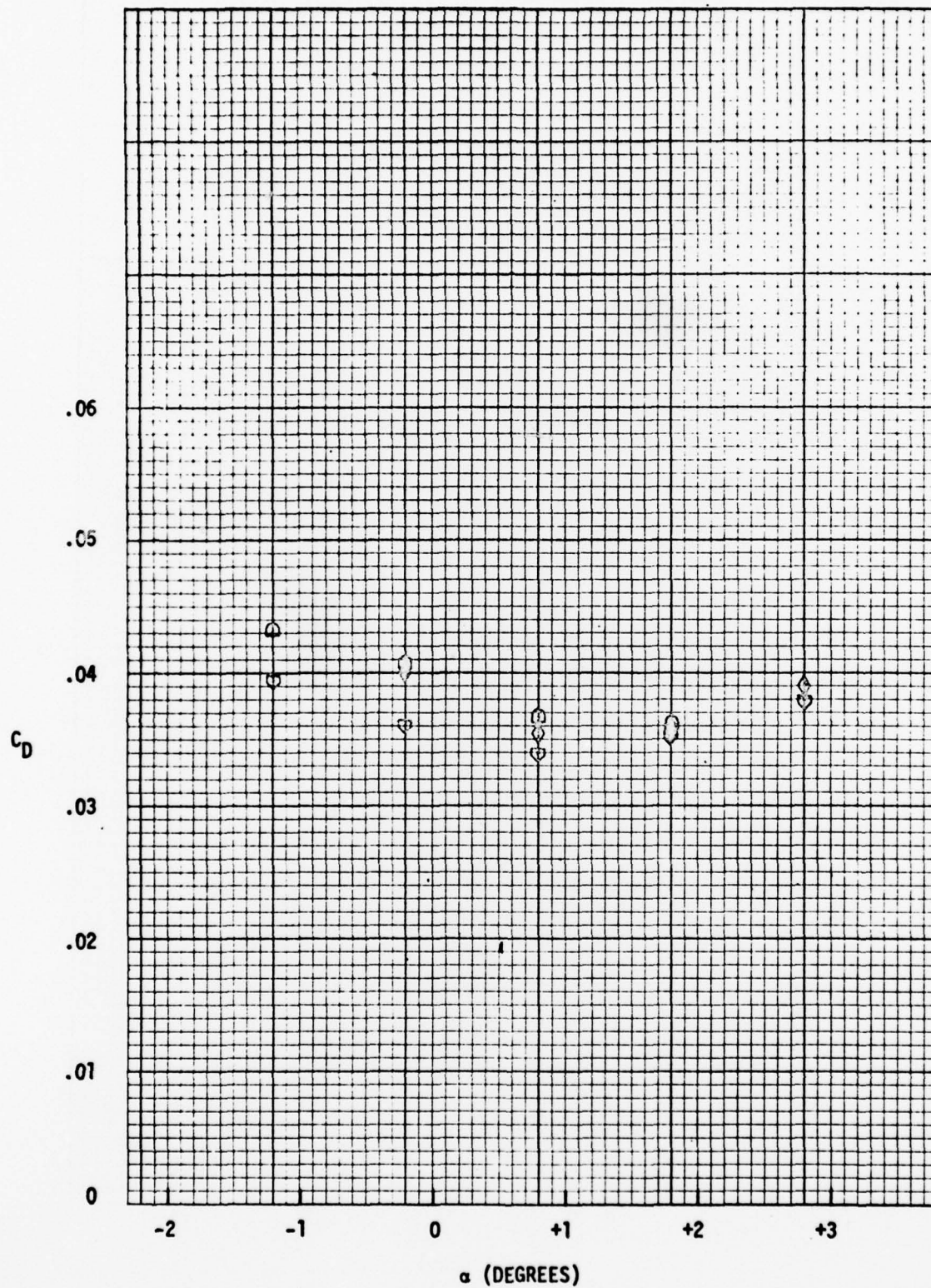
Figure 22 - Continued

62
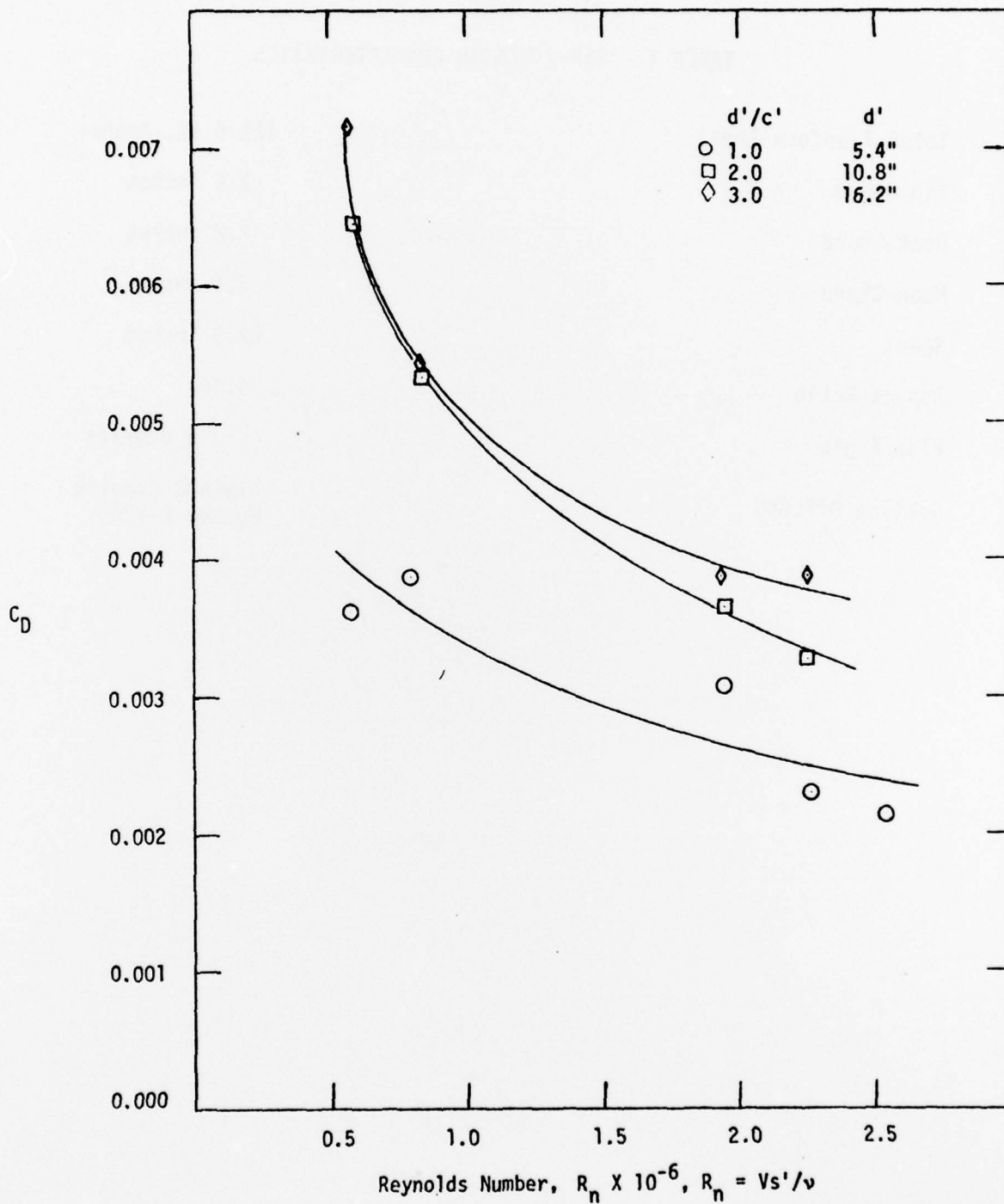
Figure 23 - Bare Strut Drag Coefficient as a Function of
Reynolds Number for the TAP-2 Strut Configuration

TABLE 1 - TAP-2 DESIGN CHARACTERISTICS

Total Planform Area	121.5 sq. inches
Tip Chord	3.6 inches
Root Chord	7.2 inches
Mean Chord	5.4 inches
Span	22.5 inches
Aspect Ratio	4.167
Flap Angle	0 degrees
Section Offsets	DTNSRDC drawing Number E-3265

TABLE 2 - TAP-2 STRUT-FOIL INCIDENCE ANGLE SETTING ARRANGEMENT

Hole Number on Strut Support Bracket	Strut Angle (β) Degrees	Foil Angle (α) Degrees
0	0	11.814
1	1	10.814
2	2	9.814
3	3	8.814
4	4	7.814
5	5	6.814
6	6	5.814
7	7	4.814
8	8	3.814
9	9	2.814
10	10	1.814
11	11	0.814
12	12	-0.186
13	13	-1.186
14	14	-2.186

TABLE 3 - TAP-2 EXPERIMENTAL CONDITIONS AND DATA

d/c'	V knots	α deg	Lift lb	Drag lb	L/D	Pitch Moment in.-lb	c_L	c_D	c_M
1.0	40.93	-2.186	527.2	157.9	3.35	-11419	.1329	.03977	-.5329
1.0	40.54	-1.186	838.9	133.6	6.29	-11447	.2156	.03433	-.5447
1.0	40.60	-0.186	1054.8	124.0	8.52	-11371	.2702	.03174	-.5393
1.0	40.70	0.814	1271.6	126.6	10.05	-11819	.3241	.03227	-.5578
1.0	40.63	1.814	1482.7	138.9	10.68	-12298	.3791	.03550	-.5823
1.0	40.25	2.814	1648.1	153.9	10.71	-12412	.4295	.04011	-.5989
1.0	44.81	-1.186	480.0	187.8	2.56	-12119	.1009	.03948	-.4718
1.0	44.94	-0.186	796.4	172.6	4.62	-12532	.1665	.03608	-.4852
1.0	45.30	0.814	1084.4	165.1	6.58	-12809	.2231	.03396	-.4880
1.0	45.29	1.814	1382.1	171.5	8.06	-13399	.2843	.03529	-.5106
1.0	45.01	2.814	1617.2	183.3	8.82	-13641	.3349	.03796	-.5231
1.0	49.94	-0.186	334.9	214.9	1.56	-12583	.0567	.03637	-.3944
1.0	49.40	0.814	835.4	200.2	4.17	-13465	.1445	.03463	-.4315
1.0	49.40	1.814	1235.3	190.4	6.49	-13907	.2137	.03294	-.4455
1.0	49.31	2.814	1565.8	201.5	7.77	-14314	.2718	.03498	-.4602
2.0	29.76	-0.186	774.3	55.8	13.91	-6541	.3690	.02661	-.5774
2.0	29.86	0.814	903.3	61.5	14.74	-6857	.4278	.02910	-.6013
2.0	30.11	1.814	987.4	70.4	14.03	-6959	.4606	.03285	-.6012
2.0	29.69	2.814	1121.0	81.9	13.70	-7412	.5308	.03877	-.6499
2.0	29.66	3.814	1130.2	87.9	12.85	-6914	.5414	.04213	-.6134
2.0	29.69	4.814	1216.2	100.5	12.10	-6933	.5822	.04813	-.6146
2.0	29.61	5.814	1344.6	119.9	11.21	-7305	.6437	.05742	-.6476
2.0	29.54	6.814	1484.7	142.5	10.42	-7687	.7183	.06894	-.6887

TABLE 3 - Continued

d/c'	V knots	α deg	Lift lb	Drag lb	L/D	Pitch Moment in.-lb	C_L	C_D	C_M
2.0	35.67	-2.186	731.8	95.9	7.64	- 9548	.2428	.03184	-.5866
2.0	35.03	-1.186	929.8	79.3	11.74	- 9155	.3200	.02728	-.5834
2.0	35.09	-0.186	1079.3	79.1	13.65	- 9233	.3700	.02712	-.5861
2.0	34.87	0.814	1257.2	90.7	13.97	- 9903	.4401	.03150	-.6368
2.0	35.04	1.814	1355.5	100.4	13.51	- 9744	.4661	.03450	-.6204
2.0	34.94	2.814	1441.4	107.8	13.38	- 9496	.4984	.03727	-.6079
2.0	34.96	3.814	1528.6	128.9	11.85	- 9834	.5280	.04450	-.6290
2.0	41.09	-2.186	471.7	176.5	2.68	-11748	.1179	.04411	-.5438
2.0	40.59	-1.186	799.5	149.9	5.34	-11925	.2049	.03840	-.5659
2.0	40.27	-0.186	1036.1	138.9	7.46	-11973	.2698	.03620	-.5773
2.0	40.95	0.814	1232.7	133.8	9.22	-11695	.3108	.03373	-.5461
2.0	40.41	1.814	1478.4	136.1	10.87	-12047	.3821	.03518	-.5766
2.0	40.73	2.814	1699.9	155.1	10.97	-12500	.4337	.03955	-.5905
2.0	44.90	-0.186	723.1	194.3	3.72	-13142	.1514	.04070	-.5096
2.0	44.62	0.814	1092.3	166.7	6.56	-12626	.2317	.03535	-.4958
2.0	44.90	1.814	1384.1	170.2	8.14	-13118	.2899	.03562	-.5087
2.0	45.05	2.814	1780.6	187.5	9.50	-14200	.3711	.03908	-.5481
3.0	29.84	-0.186	787.6	56.5	13.95	- 6610	.3728	.02676	-.5794
3.0	29.87	0.814	929.7	64.1	14.52	- 7032	.4401	.03037	-.6165
3.0	29.80	1.814	998.7	70.7	14.12	- 6996	.4748	.03361	-.6158
3.0	29.94	2.814	1131.9	83.4	13.58	- 7401	.5330	.03926	-.6453
3.0	29.66	3.814	1136.1	87.5	12.99	- 6882	.5449	.04195	-.6113
3.0	29.60	4.814	1227.1	101.4	12.10	- 6958	.5902	.04879	-.6198
3.0	29.59	5.814	1370.7	120.9	11.34	- 7417	.6610	.05828	-.6623
3.0	29.70	6.814	1543.9	146.7	10.52	- 7967	.7387	.07018	-.7059

TABLE 3 - Continued

d/c'	V knots	α deg	Lift lb	Drag lb	L/D	Pitch Moment in.-lb	C_L	C_D	C_M
3.0	34.83	-2.186	694.7	90.7	7.66	- 9011	.2418	.03158	-.5808
3.0	34.81	-1.186	899.3	80.8	11.14	- 9008	.3132	.02813	-.5809
3.0	34.96	-0.186	1073.4	80.4	13.35	- 9240	.3707	.02778	-.5910
3.0	34.88	0.814	1210.9	84.8	14.28	- 9246	.4201	.02943	-.5940
3.0	34.91	1.814	1326.8	95.6	13.88	- 9299	.4595	.03312	-.5965
3.0	35.02	2.814	1488.1	113.5	13.13	- 9988	.5123	.03907	-.6368
3.0	34.96	3.814	1547.5	131.8	11.74	-10099	.5346	.04555	-.6462
3.0	41.01	-2.186	447.8	175.5	2.55	-11619	.1125	.04406	-.5402
3.0	40.37	-1.186	800.8	149.2	5.38	-11858	.2075	.03864	-.5688
3.0	40.67	-0.186	1050.0	142.3	7.39	-12091	.2681	.03629	-.5714
3.0	40.56	0.814	1294.8	132.8	9.76	-11814	.3323	.03408	-.5614
3.0	40.48	1.814	1511.9	141.5	10.69	-12225	.3895	.03645	-.5833
3.0	44.79	-1.186	390.8	205.7	1.90	-12287	.0823	.04329	-.4789
3.0	45.17	-0.186	735.0	196.8	3.74	-13045	.1522	.04072	-.4999
3.0	45.01	0.814	1103.1	176.7	6.24	-13003	.2299	.03683	-.5018
3.0	44.87	1.814	1575.1	172.0	9.17	-13694	.3303	.03606	-.5317

TIP MODIFICATIONS

d/c'	V knots	α deg	Lift lb	Drag lb	L/D	Pitch Moment in.-lb	C_L	C_D	C_M
1.0	45.15	-1.186	444.9	193.3	2.30	-12368	.0922	.04000	-.4744
1.0	45.17	-0.186	803.4	176.0	4.58	-12782	.1665	.03648	-.4903
1.0	44.88	0.814	1114.1	161.2	6.92	-12717	.2333	.03376	-.4932
1.0	45.44	1.814	1410.7	168.6	8.37	-13281	.2885	.03448	-.5030
1.0	44.75	2.814	1752.9	176.5	9.94	-13754	.3696	.03721	-.5370

68

TABLE 3 - Continued

TIP MODIFICATIONS

d/c'	V knots	α deg	Lift lb	Drag lb	L/D	Pitch Moment in.-lb	C_L	C_D	C_M
3.0	29.98	-2.186	537.9	61.3	8.78	- 6557	.2526	.02878	-.5702
3.0	29.70	-1.186	656.1	53.8	12.18	- 6386	.3139	.02578	-.5658
3.0	29.56	-0.186	762.6	54.6	13.98	- 6511	.3685	.02638	-.5825
3.0	29.91	0.814	901.1	62.9	14.32	- 6889	.4252	.02971	-.6020
3.0	29.82	1.814	1005.2	71.1	14.15	- 7033	.4771	.03373	-.6182
3.0	29.94	2.814	1102.2	80.3	13.64	- 7212	.5189	.03805	-.6289
3.0	29.71	3.814	1147.9	88.7	12.95	- 6966	.5495	.04246	-.6175
3.0	29.75	4.814	1236.7	102.1	12.11	- 7045	.5900	.04874	-.6225
3.0	29.63	5.814	1371.9	121.0	11.34	- 7384	.6600	.05821	-.6578
3.0	29.66	6.814	1530.1	145.3	10.53	- 7873	.7345	.06974	-.6999
3.0	29.92	7.814	1828.8	186.6	9.80	- 9088	.8621	.08795	-.7934
3.0	34.89	-2.186	682.5	93.8	7.29	- 9086	.2367	.03252	-.5834
3.0	34.40	-1.186	887.3	82.6	10.75	- 9091	.3072	.02860	-.5828
3.0	35.03	-0.186	1059.6	80.8	13.11	- 9249	.3645	.02779	-.5891
3.0	34.87	0.814	1187.6	87.2	13.62	- 9299	.4119	.03026	-.5972
3.0	34.80	1.814	1317.6	98.5	13.39	- 9488	.4595	.03435	-.6128
3.0	34.81	2.814	1419.1	109.9	12.91	- 9497	.4935	.03822	-.6116
3.0	34.64	3.814	1537.6	133.5	11.53	-10871	.5404	.04691	-.7075

TABLE 3 – Continued

BARE STRUT DATA

V knots	V ft/sec	d'/c'	β deg	Drag lb	C_D	$R_n \times 10^{-6}$
10.36	17.48	1.0	-9	0.91	.00361	0.576
14.32	24.17	1.0	-9	1.89	.00388	0.797
34.89	58.88	1.0	-9	8.87	.00309	1.941
40.47	68.31	1.0	-9	8.85	.00230	2.252
45.60	76.97	1.0	-9	11.04	.00224	2.538
10.50	17.72	2.0	-9	1.68	.00645	0.584
15.00	25.31	2.0	-9	2.83	.00532	0.835
34.92	58.94	2.0	-9	10.53	.00365	1.943
40.41	68.20	2.0	-9	12.65	.00328	2.249
10.24	17.29	3.0	-9	1.78	.00717	0.570
14.98	25.29	3.0	-9	2.88	.00543	0.834
34.83	58.79	3.0	-9	11.18	.00389	1.938
40.42	68.22	3.0	-9	15.01	.00388	2.249

70

TABLE 4 - FROUDE NUMBER, REYNOLDS NUMBER AND CAVITATION
NUMBER FOR TAP-2 EXPERIMENTS

V (Knots)	Froude Number	Reynolds Number
30	13.32	1.491×10^6
35	15.54	1.740×10^6
40	17.76	1.988×10^6
45	19.98	2.237×10^6
50	22.20	2.485×10^6

V (Knots)	d/c	σ
30	1.0	.846
40	1.0	.476
45	1.0	.376
50	1.0	.304
35	2.0	.626
40	2.0	.479
45	2.0	.379
35	3.0	.635
40	3.0	.486
45	3.0	.384

DTNSRDC ISSUES THREE TYPES OF REPORTS

1. DTNSRDC REPORTS, A FORMAL SERIES, CONTAIN INFORMATION OF PERMANENT TECH-NICAL VALUE. THEY CARRY A CONSECUTIVE NUMERICAL IDENTIFICATION REGARDLESS OF THEIR CLASSIFICATION OR THE ORIGINATING DEPARTMENT.

2. DEPARTMENTAL REPORTS, A SEMIFORMAL SERIES, CONTAIN INFORMATION OF A PRELIM-INARY, TEMPORARY, OR PROPRIETARY NATURE OR OF LIMITED INTEREST OR SIGNIFICANCE. THEY CARRY A DEPARTMENTAL ALPHANUMERICAL IDENTIFICATION.

3. TECHNICAL MEMORANDA, AN INFORMAL SERIES, CONTAIN TECHNICAL DOCUMENTATION OF LIMITED USE AND INTEREST. THEY ARE PRIMARILY WORKING PAPERS INTENDED FOR IN-TERNAL USE. THEY CARRY AN IDENTIFYING NUMBER WHICH INDICATES THEIR TYPE AND THE NUMERICAL CODE OF THE ORIGINATING DEPARTMENT. ANY DISTRIBUTION OUTSIDE DTNSRDC MUST BE APPROVED BY THE HEAD OF THE ORIGINATING DEPARTMENT ON A CASE-BY-CASE BASIS.

LMED

—78